U.PORTO

MESTRADO EM ONCOLOGIA

ONCOLOGIA LABORATORIAL

Characterization of a common germline *SDHB* deletion in patients with hereditary paraganglioma-pheochromocytoma

Sara Albuquerque Pinto

M
2019

U.PORTO

Sara Albuquerque Pinto. Characterization of a common germline *SDHB* deletion in patients with hereditary paraganglioma-pheochromocytoma

M.ICBAS **2019**

Characterization of a common germline
SDHB deletion in patients with hereditary
paraganglioma-pheochromocytoma
Sara Albuquerque Pinto

INSTITUTO DE CIÊNCIAS BIOMÉDICAS ABEL SALAZAR

SARA DANIELA ALBUQUERQUE PINTO

CHARACTERIZATION OF A COMMON GERMLINE *SDHB* DELETION IN PATIENTS WITH HEREDITARY PARAGANGLIOMA-PHEOCHROMOCYTOMA

Dissertação de Candidatura ao grau de Mestre em Oncologia – especialização em Oncologia Laboratorial – submetida ao Instituto de Ciências Biomédicas de Abel Salazar da Universidade do Porto.

Orientador:
Manuel António Rodrigues Teixeira, MD, PhD
Diretor do Serviço de Genética e Centro de Investigação
Instituto Português de Oncologia do Porto
Professor Catedrático Convidado do Departamento de Patologia e Imunologia Molecular
Instituto de Ciências Biomédicas de Abel Salazar da Universidade do Porto

Coorientador:
Manuela Cristina Dias Pinheiro, PhD
Investigador Postdoc
Serviço de Genética e Centro de Investigação – Grupo de Oncogenética
Instituto Português de Oncologia do Porto

Agradecimentos

Em primeiro lugar gostaria de demonstrar o meu agradecimento ao Professor Manuel Teixeira, meu orientador e professor, por me ter permitido realizar este trabalho no local que escolhi, o Serviço de Genética do IPO do Porto. Obrigada pela simpatia, atenção, disponibilidade e transmissão de conhecimentos.

À minha coorientadora, Manela, a pessoa mais dedicada, trabalhadora e inteligente que, muito sinceramente, tive o privilégio de conhecer! Um agradecimento igualmente especial à Anita, a quem quero agradecer toda a disponibilidade, ajuda e compreensão. É gratificante trabalhar e aprender convosco.

À Carla, Catarina, Joana, João, Pedro e Susana pela amizade, pela companhia nas horas de almoço, pela partilha de momentos divertidos, pelo carinho e ajuda. Todos, sem exceção, contribuíram para o meu crescimento pessoal e profissional.

À Professora Dr.ª Carmen Jerónimo, atual diretora do Mestrado, e a todos os docentes com os quais adquiri conhecimento ao longo destes dois últimos anos.

A todos os elementos do Serviço de Genética do IPO do Porto, pelos bons momentos partilhados, pela simpatia e ajuda.

Aos meus amigos e família pelo incentivo e força desde o início desta aventura.

“Our greatest weakness lies in giving up. The most certain way to succeed is always to try just one more time.”

(Thomas A Edison)

TABLE OF CONTENTS

Table of contents

Figure index 13

Table index 17

List of abbreviations 21

Abstract 27

Resumo 31

I. Introduction 35

1. Anatomy and Physiology of the Autonomic Nervous System (ANS) 35

2. Pheochromocytoma and Paraganglioma 36

3. Epidemiology 38

4. Biochemical Phenotype, Signs and Symptoms 38

5. Diagnosis, Treatment and Follow-up 40

6. Tumorigenesis 41

6.1 Pseudohypoxic Signaling Cluster 42

6.2 Kinase Signaling Cluster 43

6.3 Wnt Signaling Cluster 45

7. Hereditary Pheochromocytoma and Paraganglioma (HPPGL) 45

7.1 Syndromic Forms 46

7.1.1 Multiple Endocrine Neoplasia type 2 47

7.1.2 von Hippel-Lindau disease 47

7.1.3 Neurofibromatosis type 1 48

7.1.4 Multiple Endocrine Neoplasia type 1 49

7.1.5 Hereditary Leiomyomatosis and Renal Cell Carcinoma syndrome 49

7.2 Other Susceptibility Genes Described for Hereditary PPGL 49

7.3 Hereditary PPGL Related to *SDHx* 50

7.3.1 Hereditary PPGL related to *SDHD* (PGL type 1) 51

7.3.2 Hereditary PPGL related to *SDHAF2* (PGL type 2) 51

7.3.3 Hereditary PPGL related to *SDHC* (PGL type 3) 52

7.3.4 Hereditary PPGL related to *SDHB* (PGL type 4) 52

7.3.5 Hereditary PPGL related to *SDHA* (PGL type 5) 52

7.4 *SDHB* Exon 1 Deletion 53

II. Aims 57

III. Materials and Methods 61

1. Clinical Samples 61

2. *SDHB* Exon 1 Germline Deletion Breakpoint Identification................................61

3. *SDHB* Exon 1 Deletion Specific Assay...63

4. *SDHB* Exon 1 Deletion Genomic Breakpoints and Sequence Context Analysis.64

5. Haplotype Analysis 64

5.1 Microsatellite Genotyping...65

5.2 Haplotype Construction and Estimation of Mutation Age 66

5.3 SNPs Markers Genotyping 66

6. Penetrance of all Clinical Manifestations Related to *SDHB* Exon 1 Deletion......67

IV. Results 71

1. Characterization of Hereditary PPGL Families..71

2. *SDHB* Exon 1 Deletion Breakpoint Identification and Characterization 73

3. Haplotype Analysis and Estimation of Mutation Age 74

4. Penetrance of all Manifestations Related to *SDHB* Exon 1 Deletion 75

V. Discussion...81

VI. Conclusions 89

VII. Future Perspectives..93

VIII. References 97

FIGURE INDEX

Figure index

Figure 1 - Organization of autonomic nervous system neurons. Adapted from Seeley et al. (2006b) 36

Figure 2 - Illustrative representation of sympathetic paragangliomas (on the left) and parasympathetic paragangliomas (on the right) anatomical location. Adapted from Katabathina et al. (2019). 37

Figure 3 - Normoxia cellular state with hypoxia pathway inhibition and consequent proteasomal degradation of HIFs (on the left). Hypoxia or pseudoxypoxia cellular state with activation of the hypoxia pathway, stabilization of HIFs and consequent transcription of target genes, promoting tumorigenesis (on the right). Adapted from Gupta et al. (2017)..43

Figure 4 - Schematic representation of the kinase signaling cluster genes and signaling pathways**.** Adapted from Katabathina et al. (2019). 44

Figure 5 - Illustration of the mitochondrial succinate dehydrogenase enzyme (or complex II of the electron transport chain), including the four subunits (SDHA, B, C, D) and the SDHAF2 cofactor**.** Adapted from Ricketts et al. (2012). 50

Figure 6 - Pedigrees of two HPPGL families presenting the *SDHB* exon 1 deletion, namely family #7 (A) and family #8 (B). 71

Figure 7 - Geographic origin of the families presenting the *SDHB* exon 1 germline deletion in Portugal. Black circles and the number within represent the families and its frequency. On the left, the larger-scale map represents Braga (upper) and Porto (lower) districts.....73

Figure 8 - Molecular characterization of the *SDHB* c.-151-10260_73-3865del mutation by a PCR specific assay and sequencing analysis. (A) Genomic DNA analysis by a three primer set amplification. The positive cases (lane 5 and 6) present two bands corresponding to a 351 bp amplicon from the wild-type allele and an additional 290 bp long amplicon from the mutated allele; the negative cases (lane 1 to 4) present only the 351 bp amplicon from the wild-type alleles. NTC is a non-template control and MW refers to 100 bp DNA standard. (B) Sequence electropherograms of the normal (upper) and mutated (lower) alleles in the

SDHB exon 1 deletion breakpoint region. The overlapping region indicates a 3 bp homology sequence (CTG) shared by the 5’ and 3’ breakpoint flanking regions. The deletion of four nucleotides (AATA) in *SDHB* intron 1 is also indicated (black arrow). 74

Figure 9 - Penetrance estimates of all manifestations (PPGLs, RCC and GIST) of the *SDHB* exon 1 deletion including probands (A) and excluding probands (B). 76

TABLE INDEX

Table index

Table 1 - Genes associated with HPPGL, chromosomal locus, associated syndrome, germline pathogenic variants prevalence and mode of inheritance. Adapted from Muth et al. (2019). 46

Table 2 - Gross deletions involving *SDHB* exon 1 described in the literature until August 2019. 54

Table 3 - PCR program used for the detection of the *SDHB* exon 1 deletion. 62

Table 4 - PCR program used for the sequencing reaction. 63

Table 5 - Microsatellite markers used for haplotype analysis and respective repeat unit, genomic location and primer sequences. 65

Table 6 - Primers used for single nucleotide polymorphisms analysis. 67

Table 7 - Clinicopathological features of the 24 probands, studied at the Portuguese Oncology Institute of Porto, and 8 affected relatives. 72

Table 8 - Microsatellite markers and SNP haplotypes of the 12 informative and 12 non-informative *SDHB* exon 1 deletion positive families. 77

LIST OF ABBREVIATIONS

List of abbreviations

ANS	Autonomic nervous system
BAP1	BRCA1 associated protein 1
BKP	Breakpoint
CNS	Central nervous system
CNV	Copy number variation
CSDE1	Cold shock domain containing E1
CT	Computed tomography scan
DNA	Deoxyribonucleic acid
dNTP	Deoxynucleoside triphosphate
ddNTP	Dideoxynucleoside
EGLN1/PHD2	EGL-9 family hypoxia inducible factor 1
EGLN2/PHD1	EGL-9 family hypoxia inducible factor 2
ETC	Electron transport chain
FDG	Fluorodeoxyglucose
FH	Fumarate hydratase
FMTC	Familial medullary thyroid cancer
GIST	Gastrointestinal stromal tumors
GLUT1	Glucose transporter 1
HIFs	Hypoxia inducible factors
HPPGL	Hereditary pheochromocytoma and paraganglioma
HR	Homologous recombination
KIF1B	Kinesin family member 1B
KIT	KIT proto-oncogene, receptor tyrosine kinase
KMT2D	Lysine methyltransferase 2D
LOVD	Leiden Open Variation Database
MAML3	Mastermind like transcriptional coactivator 3
MAX	MYC associated factor X
MDH2	Malate dehydrogenase 2
MEN1	Menin 1
MIBG	Metaiodobenzylguanidine
MLPA	Multiplex ligation probe amplification
MRI	Magnetic resonance imaging
MTC	Medullary thyroid carcinoma
mTOR	Mammalian target of rapamycin

MUT	Mutated allele
MXD1	Max dimerization protein 1
MYC	MYC proto-oncogene
NAHR	Non-allelic homologous recombination
NCCN	National Comprehensive Cancer Network
NF1	Neurofibromin 1
OMIM	Online Mendelian Inheritance in Man
^{177}Lu-PRRT	^{177}Lutethium Peptide Receptor Radionuclide Therapy
PA	Pituitary adenoma
PCR	Polymerase chain reaction
PDGF	Platelet-derived growth factor
PDGFRA	Platelet-derived growth factor receptor alpha
PET	Positron emission tomography
PHD	HIF prolyl-hydroxylase
PI3K	Phosphoinositide 3-kinase
PNS	Peripheral nervous system
PHEO	Pheochromocytoma
PGL	Paraganglioma
PPGLs	Pheochromocytoma and paraganglioma
RET	Ret proto-oncogene
RCC	Renal cell carcinoma
SDHA	Succinate dehydrogenase complex flavoprotein subunit A
SDHAF2	Succinate dehydrogenase complex assembly factor 2
SDHB	Succinate dehydrogenase complex iron sulfur subunit B
SDHC	Succinate dehydrogenase complex subunit C
SDHD	Succinate dehydrogenase complex subunit D
SDHx	Succinate dehydrogenase group of genes (*SDHA,B,C* and *D*)
SINEs	Short interspersed nuclear elements
SNP	Single-nucleotide polymorphism
TCF4	Transcription factor 4
TGFα	Transforming growth factor alpha
TMEM127	Transmembrane protein 127
UBTF	Upstream binding transcription factor, RNA polymerase I
UCSC	University of California, Santa Cruz
VEGF	Vascular endothelial growth factor
VHL	von Hippel-Lindau tumor suppressor

WHO	World Health Organization
WT	Wild-type

ABSTRACT

Abstract

Pheochromocytoma and paraganglioma (PPGL) are rare neuroendocrine tumors of the autonomic nervous system. According to their anatomical location, they can be divided into two main groups: sympathetic paragangliomas (including pheochromocytomas) and parasympathetic paragangliomas. About 40% of PPGL arise in the context of hereditary disease, associated with germline mutations in several genes. Hereditary PPGL (HPPGL) can be caused by mutations in the *SDHB* gene, a member of the succinate dehydrogenase enzyme. Although the mutational spectrum of the *SDHB* gene mainly includes missense and nonsense mutations, a significant amount of HPPGL patients present large genomic rearrangements. Particularly, one *SDHB* exon 1 deletion has been reported recurrently in HPPGL families from the north of the Iberian Peninsula and has been associated with a founder effect. A high frequency of families presenting a *SDHB* exon 1 deletion were identified at the Portuguese Oncology Institutes of Porto, Coimbra and Lisbon. The aims of this national level study were: to characterize the genomic breakpoints of all the *SDHB* exon 1 deletions; to perform haplotype studies in order to determine if it is a founder mutation in the Portuguese families; to estimate the age of the mutation; to determine the geographical distribution of the families presenting this rearrangement; and to estimate the penetrance of the disease in these families.

This study included 30 HPPGL families presenting a *SDHB* exon 1 deletion previously detected by Multiplex Ligation Probe Amplification (MLPA). Twenty-four, four and two families were studied by routine genetic diagnosis at the Portuguese Oncology Institutes of Porto, Lisbon and Coimbra, respectively. We performed PCR specific amplification and Sanger sequencing in all positive samples, and all the cases harbored an identical deletion of 15,678 bp, corresponding to the *SDHB* variant c.-151-10260_73-3865del (HGVS, NC_000001.11 (SDHB): ATG=1). Haplotype analysis was performed using microsatellite markers flanking the *SDHB* gene. Nine different haplotypes were phased for 12 informative families and a conserved region of approximately 47 kb was observed. All families also shared the SNPs haplotype previously described by Martins et al., (2013) and most families were originated from the north region of Portugal. The penetrance of the disease was estimated using data from 78 *SDHB* exon 1 deletion carriers, including 22 probands and 56 family members. The penetrance estimation was 66.2% and 29.4% at the age of 75 years, including and excluding probands, respectively, which is similar to that observed for other *SDHB* mutations.

Concluding, all *SDHB* exon 1 deletion carriers presented the same 15,678 bp deletion, previously described as the Iberian founder deletion. Microsatellite haplotype analysis revealed a conserved region of about 47 kb, indicating a possible common origin for the Portuguese families. To our knowledge, this is the first study to characterize the genomic breakpoints of families presenting the *SDHB* exon 1 deletion at the national level and to perform an extensive microsatellite haplotype analysis. Nonetheless, additional studies including all families reported worldwide would be important to further evaluate the ancestral origin and the age of this mutation.

RESUMO

Resumo

Feocromocitomas e paragangliomas (FEO/PGLs) são tumores neuroendócrinos do sistema nervoso autónomo. De acordo com a sua localização anatómica, podem ser divididos em dois grupos principais: paragangliomas simpáticos (incluindo os feocromocitomas) e parassimpáticos. Cerca de 40% dos FEO/PGLs ocorrem no contexto de síndrome hereditária, associados com mutações germinativas em vários genes. Os FEO/PGLs hereditários podem ser causados por mutações no gene *SDHB*, um membro da enzima sucinato desidrogenase. Apesar do espetro mutacional do gene *SDHB* incluir maioritariamente mutações *missense* e *nonsense*, uma parte significativa de doentes apresentam rearranjos genómicos. Especificamente, uma deleção do exão 1 do gene *SDHB* tem sido frequentemente descrita em famílias diagnosticadas com FEO/PGLs, oriundas da região norte da península ibérica, tendo sido associada a um efeito fundador. Uma elevada frequência de famílias apresentando a deleção do exão 1 do gene *SDHB* foram identificadas nos Institutos Portugueses de Oncologia do Porto, de Coimbra e de Lisboa. Este trabalho teve como objetivos: caracterizar o ponto de quebra genómico das deleções do exão 1 do gene *SDHB* identificadas em famílias Portuguesas; efetuar estudos de haplótipo de forma a avaliar se este rearranjo é uma mutação fundadora em Portugal; estimar a idade desta mutação; determinar a distribuição geográfica das famílias com esta alteração; e estimar a penetrância da doença nos portadores.

O estudo incluiu 30 famílias diagnosticadas com FEO/PGL hereditário e que apresentavam a deleção do exão 1 do gene *SDHB* previamente detetada por MLPA (Multiplex Ligation Probe Amplification). Vinte e quatro, quatro e duas famílias foram identificadas no âmbito do diagnóstico genético da síndrome nos Institutos Portugueses de Oncologia do Porto, Lisboa e Coimbra, respetivamente. De forma a identificar os pontos de quebra, efetuamos PCR específico para a deleção e sequenciação de Sanger em todas as amostras previamente consideradas positivas, e todos os casos apresentaram uma deleção de 15,678 bp, correspondente à variante *SDHB* c.-151-10260_73-3865del (HGVS, NC_000001.11 (SDHB): ATG=1). O estudo de haplótipo foi efetuado usando marcadores microssatélite a flanquear o gene *SDHB*. Nove haplótipos diferentes foram observados em 12 famílias informativas e uma região conservada de aproximadamente 47 kb foi identificada. Adicionalmente, todas as famílias também apresentaram o haplótipo usando SNPs previamente descrito por Martins et al., (2013) e a origem geográfica da maioria das famílias é a região norte de Portugal. A penetrância foi estimada recorrendo a dados de 78 portadores da deleção do exão 1 do gene *SDHB*, incluindo 22 casos índice e 56 familiares.

A penetrância estimada foi de 66.2% e 29.4% aos 75 anos de idade, incluindo e excluindo os casos índice da análise, respetivamente, sendo semelhante à observada para outras mutações do mesmo gene.

Concluindo, todos os portadores da deleção do exão 1 do gene *SDHB* apresentaram a mesma deleção de 15,678 bp, previamente descrita como a deleção fundadora da Península Ibérica. O estudo de haplótipos usando marcadores microssatélite revelou uma região conservada de aproximadamente 47 kb, sugerindo um ancestral comum para as famílias portuguesas. Tanto quanto é do nosso conhecimento, este é o primeiro estudo a caracterizar o ponto de quebra de famílias com uma deleção do exão 1 do gene *SDHB* a nível nacional e a efetuar uma extensa análise de haplótipos usando marcadores microssatélites. No entanto, estudos adicionais incluindo todas as famílias reportadas mundialmente seriam importantes para avaliar a origem ancestral e a datação desta mutação.

I. INTRODUCTION

I. Introduction

Cancer is generally considered a large group of diseases characterized by uncontrolled cell division, resistance to cell death, invasion of adjacent tissues and, eventually, dissemination to other organs (Hanahan and Weinberg, 2011). According to GLOBOCAN worldwide data from 2018, there were 18.1 million new cancer cases and 9.6 million cancer deaths (including nonmelanoma skin cancer), which makes cancer the second leading cause of death globally (Ferlay et al., 2019). Incidence and mortality related to cancer are growing worldwide, reflecting aging of the population as well as changes in risk factors prevalence and distribution (i.e. smoking, western diet and physical inactivity) (Bray et al., 2018).

1. Anatomy and Physiology of the Autonomic Nervous System (ANS)

By definition, the nervous system is divided into central (CNS) and peripheral nervous system (PNS). The CNS includes the brain and spinal cord. The PNS consists of ganglia, nerves, sensory receptors and plexuses and it can be subdivided into the afferent and the efferent division. The afferent division is responsible for transmitting the action potentials from the sensory receptors to the CNS. The efferent division does the opposite, transmitting the action potentials from the CNS to the effector organs, such as glands. The efferent division includes the somatic nervous system and the autonomic nervous system (ANS). Specifically, ANS includes the sympathetic and parasympathetic divisions, and the enteric nervous system, controlling involuntarily or subconsciously certain glands, smooth and cardiac muscle (Wehrwein et al., 2016). Within the ANS, efferent signals between the CNS and the effector organ are transmitted by preganglionic and postganglionic neurons, and the autonomic ganglia (Seeley et al., 2006b) (Figure 1). The preganglionic neurons (whose cell bodies are located in the CNS) synapse with the postganglionic neurons, within the autonomic ganglia (where the cell bodies of the postganglionic neurons are located, and the preganglionic neuron axons extend); and the axons of the postganglionic neurons extend to the effector organ. The ANS sympathetic and parasympathetic divisions differ in the location of their preganglionic neuron cell bodies within the CNS, and the location of their autonomic ganglia (Seeley et al., 2006a).

The sympathetic division has its preganglionic neuron cell bodies located between the first thoracic (T1) and the second lumbar (L2) segments. The autonomic ganglia are called sympathetic chain ganglia (or paravertebral ganglia), being located along the two sides of the vertebral column (Wehrwein et al., 2016). Specifically for the adrenal glands, the axons of the preganglionic neurons synapse directly with cells in the adrenal medulla, the inner portion of that gland. The adrenal medulla is composed by a group of cells which derived from the neural crest, during the embryonic development, as well as postganglionic cells of the ANS (Seeley et al., 2006a).

The preganglionic neuron cell bodies of the parasympathetic division are located in the brainstem or in the sacral zone of the spinal cord, between the S2 and S4. Their axons are in cranial and pelvic nerves and synapse with the postganglionic neuron, within the terminal ganglia (Seeley et al., 2006a).

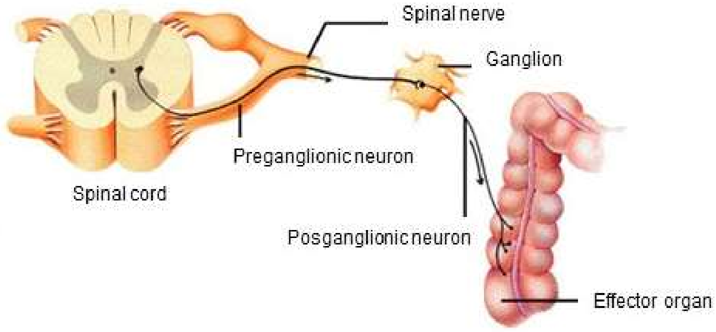

Figure 1 - Organization of autonomic nervous system neurons. Adapted from Seeley et al. (2006b)

2. Pheochromocytoma and Paraganglioma

Pheochromocytomas and paragangliomas (PPGLs) are highly vascular neuroendocrine tumors of the ANS (Lenders et al., 2005). According to the fourth edition of the WHO classification of endocrine tumors, PPGLs are classified as tumors of the adrenal medulla and extra-adrenal paraganglia, based on their location or origin (Lam, 2017). More specifically, paragangliomas (PGLs) arise from neural crest-derived paraganglion cells, located in the ANS sympathetic or parasympathetic ganglia and accompanying nerves (Lenders et al., 2014; Lam, 2017). Pheochromocytomas (PHEOs) arise from adrenal medulla chromaffin cells, being therefore considered as intra-adrenal sympathetic PGLs (Lam, 2017).

Based on the clinical and biological behavior, PGLs can be divided in two groups: sympathetic and parasympathetic PGLs. Sympathetic PGLs from the adrenal medulla represent about 80-85% of the cases and, the remaining 15-20% are extra-adrenal, located in the prevertebral and paravertebral sympathetic ganglia of the chest, abdomen (most commonly from the organ of Zuckerkandl, a chromaffin tissue situated near the mesenteric artery) and pelvis (Pacak and Tella, 2000; Lenders et al., 2005) (Figure 2). Parasympathetic PGLs are mainly located in the head and neck, being therefore also known as head-and-neck PGLs (Lam, 2017). According to the anatomical sites of origin, parasympathetic PGLs could be subdivided into four groups: carotid body, jugulotympanic (middle ear), vagal and laryngeal PGLs (Chan JKC et al., 2017) (Figure 2). Carotid body location represents more than 50% of the total parasympathetic PGLs (Lam, 2017).

Considering the fourth edition of the WHO classification of endocrine tumors, the "malignant PPGL" terminology must be replaced by "metastatic PPGL" (Lam, 2017). This was justified by the fact that there is no histological system validated and universally adopted for the establishment of the biological aggressiveness of the tumor (Lam, 2017). Although the majority of PPGLs are benign tumors, approximately 10% of PHEOs and 25% of PGLs are metastatic, usually found in lungs, liver, bones and lymph nodes (Pacak and Tella, 2000).

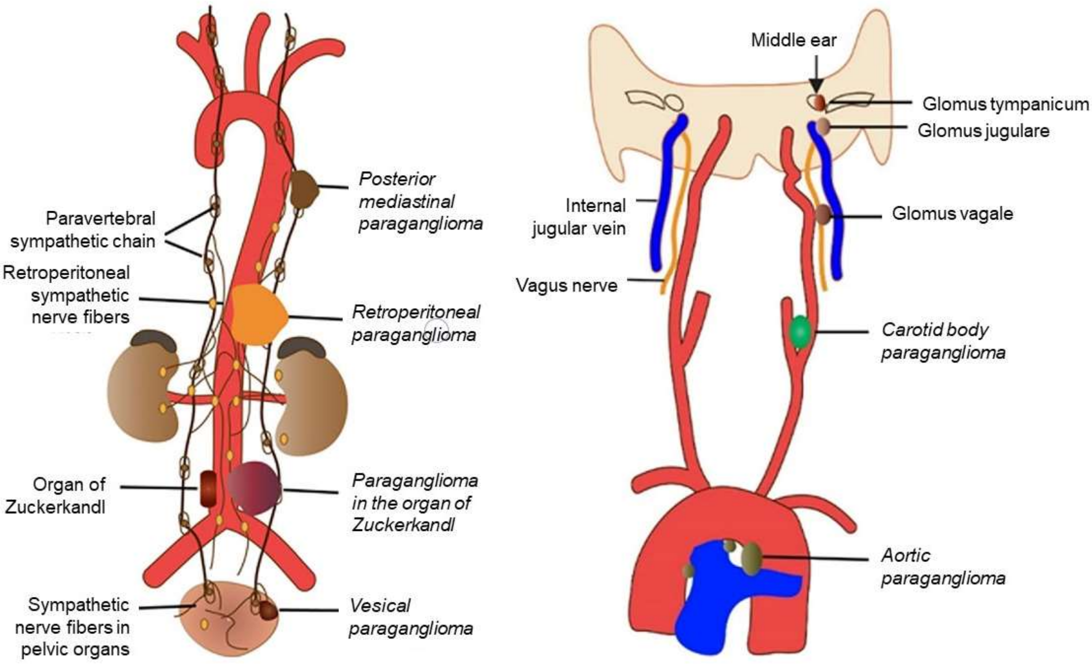
Paravertebral sympathetic chain
Retroperitoneal sympathetic nerve fibers
Organ of Zuckerkandl
Sympathetic nerve fibers in pelvic organs
Posterior mediastinal paraganglioma
Retroperitoneal paraganglioma
Paraganglioma in the organ of Zuckerkandl
Vesical paraganglioma
Middle ear
Glomus tympanicum
Glomus jugulare
Internal jugular vein
Glomus vagale
Vagus nerve
Carotid body paraganglioma
Aortic paraganglioma

Figure 2 - Illustrative representation of sympathetic paragangliomas (on the left) and parasympathetic paragangliomas (on the right) anatomical location. Adapted from Katabathina et al. (2019).

3. Epidemiology

PPGLs are considered rare tumors, irrespective of arising in the context of sporadic or hereditary disease. For the general population, the reported annual incidence is 3 to 8 cases per 1 million, and the estimated annual prevalence is 1:4,500 and 1:1,700 for PHEO and PGL, respectively (Pacak et al., 2001). In a recent study performed on a vast cohort of patients from the Netherlands, the observed incidence was 0.57 per 100,000 persons-year considering the period between 2011 and 2015 (Berends et al., 2018). In the United States, the reported annual incidence rate in 2014 was 0.8 per 100,000 persons-years (Shuch et al., 2014). However, the incidence of PPGLs can be higher, if we account the number of tumors diagnosed during autopsy procedures (Lenders et al., 2014). In Portugal, the National Oncology Registry (RON) from 2010, reported an incidence rate for adrenal-gland tumors (in which PHEO is included) of 0.2 per 100,000 malignant tumors and an incidence rate for endocrine glands tumors (in which PGL is included) of 0.1 per 100,000 malignant tumors (RORENO, 2016).

The peak incidence occurs between the third and the fifth decades, however these tumors are diagnosed earlier when associated with a hereditary predisposition (Eisenhofer et al., 2011). PPGLs are a rare cause of secondary arterial hypertension (HTA), occurring on approximately 0.1% of hypertensive patients (Pacak and Tella, 2000).

The only environmental risk factor described so far is the exposure to chronic hypoxia, i.e. living at high altitudes is associated with increased incidence of head-and-neck paraganglioma (Astrom et al., 2003; Cerecer-Gil et al., 2010; Favier and Gimenez-Roqueplo, 2010; Waguespack et al., 2010; Opotowsky et al., 2015; Cascon et al., 2019).

4. Biochemical Phenotype, Signs and Symptoms

PPGLs are neuroendocrine tumors and catecholamine secretors. Catecholamines, including adrenaline (or epinephrine), noradrenaline (or norepinephrine) and dopamine, are hormones produced by the chromaffin cells of the adrenal medulla and the postganglionic fibers of the sympathetic nervous system (thoracic and abdominal locations) (Dahia, 2014). Metanephrine, normetanephrine and 3-methoxytyramine are adrenaline, noradrenaline and dopamine metabolites, respectively, and all of them are considered for establishing the tumor's biochemical phenotype (Else et al., 2018; NCCN, 2019). Therefore, PPGLs can be classified into three different biochemical phenotypes: noradrenergic, adrenergic and dopaminergic (Gupta et al., 2017). The noradrenergic phenotype includes PPGLs that are characterized by elevated levels of norepinephrine and normetanephrine and is suggestive for the presence of mutations in *VHL*, *SDHx*, *FH*, *MDH2*, *EPAS1/HIF2A* and *SDHAF2* genes (Pacak and Tella, 2000; Gupta et al., 2017). The majority of the tumors included in this biochemical phenotype are located outside the adrenal gland, but, PHEOs can also show a noradrenergic phenotype, namely when they occur in the context of von Hippel-Lindau (VHL) syndrome (Pacak and Tella, 2000). The adrenergic phenotype includes PPGLs characterized by elevated levels of epinephrine and norepinephrine and the tumor location is typically on the adrenal glands, although tumors with *TMEM127* mutations are an exception (Pacak and Tella, 2000; Gupta et al., 2017). The PPGLs with this biochemical phenotype usually harbor mutations in kinase signaling related genes, such as *NF1, RET, TMEM127* and *MAX* (Pacak and Tella, 2000). The dopaminergic phenotype includes PPGLs characterized by elevated levels of dopamine, but slightly elevated levels of norepinephrine/normetanephrine can also be present. This phenotype can occur with some head-and-neck PGLs (more specifically, carotid body PGLs) and its characteristic of metastatic disease, especially in *SDHB* and *SDHD* mutated tumors (Pacak and Tella, 2000). Therefore, the biochemical phenotype can be suggestive of the tumor anatomical location (Turchini et al., 2018).

Hypertension (continuous, intermittent or paroxysmal) is the most common feature of PHEOs and sympathetic PGLs (Parenti et al., 2012). Hypertensive crises are associated with severe headaches, diaphoresis and palpitations. Dyspnea, weakness, arrythmias, weakness, glucose intolerance and weight loss are other symptoms associated with catecholamine hypersecretion (Lenders et al., 2005; Fishbein, 2019). The high morbidity and mortality are essentially related with cardiovascular events, such as sudden death, myocardial infarction and cerebrovascular accidents (Lenders et al., 2005; Parenti et al., 2012).

Parasympathetic PGLs are usually associated with the tumor mass effect and infiltration of adjacent structures (Fishbein, 2019). Palpable neck masses, dysphagia, tinnitus and cranial nerve palsies could be observed in some patients with this type of tumor (Erickson et al., 2001; Fishbein, 2019). Indeed, catecholamine hypersecretion is absent in 95% of these head-and-neck tumors; the remaining 5% are either a subset of carotid body tumors or arise from the cervical sympathetic chain (Pacak and Tella, 2000; Else et al., 2018).

5. Diagnosis, Treatment and Follow-up

The disease diagnosis is based on evaluation of the catecholamine hypersecretion by biochemical testing, and localization of the tumor by imaging methods. Both are equally important; however, the first approach should be the biochemical testing, followed by imaging studies (Pacak and Tella, 2000; Lenders et al., 2014). The biochemical diagnosis of secreting PPGLs is based on catecholamines and respective metabolites levels, which can be evaluated in plasma or urine samples (specifically, plasma free metanephrines or urinary fractionated metanephrines). Liquid chromatography with mass spectrometric or electrochemical detection methods should be the election methods for establishing the biochemical diagnosis (Lenders et al., 2014). The concomitant use of certain drugs (including acetaminophen, some β- and α-adrenoreceptor blocking drugs, serotonin-reuptake inhibitors and monoamino oxidase inhibitors), as well as caffeine and alcohol intake, smoking, and strenuous physical activity in the 24 hours prior to testing, can cause false-positive test results (Neary et al., 2011; Hannah-Shmouni et al., 2017). False-negative metanephrine test results could occur in presence of head-and-neck, nonfunctional or small (less than 1 cm) tumors (Gupta et al., 2017). For dopaminergic phenotype tumors, like some head-and-neck paragangliomas, it is recommended to test the dopamine metabolite 3-methoxytyramine and not dopamine itself, because most of urine dopamine is formed in renal cells (Eisenhofer et al., 2005).

In terms of imaging methods used for diagnosis, chest computed tomography (CT)-scans (with or without contrast) and abdominal/pelvic multiphasic CT or magnetic resonance imaging (MRI) scans are also recommended. However, CT is the recommended first-choice, because it offers better spatial resolution for anatomical locations such as the abdomen, thorax and pelvis (Lenders et al., 2014; NCCN, 2019). If metastatic disease is suspected, MRI is the recommended method, although other imaging studies could be performed (including somatostatin receptor-based imaging, Fluorodeoxyglucose - Positron emission tomography (FDG-PET)/CT, Metaiodobenzylguanidine (MIBG) scan, and bone scan) (Lenders et al., 2014; NCCN, 2019).

Genetic testing is also recommended for all patients with PPGL, regardless of patient and family characteristics and should be performed using a clinical feature-driven diagnostic algorithm to establish the priorities for specific genetic testing, according to a syndromic or metastatic presentation (Lenders et al., 2014; Plouin et al., 2016; Fishbein, 2019; Muth et al., 2019; NCCN, 2019). A young age at diagnosis, presence of positive family history, and presentation of multifocal tumors or bilateral pheochromocytomas are prioritizing features for patients genetic testing. Tumor location and biochemical phenotype considerations are also helpful for guiding genetic testing (Lenders et al., 2014). The identification of a hereditary syndrome in the proband may result in earlier diagnosis and treatment of PPGLs in the family members (Lenders et al., 2014).

The definitive treatment of PPGLs is surgical resection, using a laparoscopic approach, whenever possible. However, for secreting tumors, a pre-operative medical management is essential to prevent perioperative cardiovascular complications (such as arrythmias and hypertensive crises), which can arise from the exposure to high circulating catecholamine levels during the surgical procedure (Berruti et al., 2012; Lenders et al., 2014; Fishbein, 2019; NCCN, 2019). This pre-operative management generally includes, in first line, the use of α-adrenergic receptor block drugs (known as “alpha blockade”) with an aggressive volume repletion and a high-sodium diet during 10-14 days or until stabilization of blood pressure and heart rate (Lenders et al., 2014; NCCN, 2019). If necessary, other drugs can be used after the alpha blockade. When the tumor is locally unresectable, the medical therapy for secreting tumors must be continued, in addition to one of the following four options: cytoreductive resection, radiotherapy, iodine-131-MIBG or ^{177}Lutethium Peptide Receptor Radionuclide Therapy (^{177}Lu-PRRT). For metastatic disease, the aim of the treatment is to control the excessive catecholamine secretion and tumor burden, however, no curative approach is achievable (Berruti et al., 2012; NCCN, 2019; Pang et al., 2019).

The recommended lifelong surveillance for PPGL patients includes biochemical, imagiological and clinical examination. Eventually, if a pathogenic variant in a susceptibility gene is found, the type and frequency of the surveillance measures should be based on the genotype-phenotype relationships established for the affected gene (Fishbein, 2019).

6. Tumorigenesis

The tumorigenesis mechanism of PPGLs it’s quite diverse, involving a great variety of biological pathways, related to somatic and germline genetic alterations. PPGLs can be segregated into three clusters, according to their transcription profile: genes associated with metabolic reprogramming and pseudo-hypoxic signaling; kinase signaling and protein translation; and the Wnt-signaling pathway (Jochmanova and Pacak, 2018; Pang et al., 2019).

6.1 Pseudohypoxic Signaling Cluster

The tumors included in this group typically present a metabolic reprogramming and pseudohypoxic signature, commonly linked to mutations in *VHL, SDHx (SDHA, SDHB, SDHC, SDHD), SDHAF2, HIF2A, EGLN1/2, MDH2* and *FH* genes (Jochmanova and Pacak, 2018). This cluster is characterized by upregulation of hypoxia inducible factors (HIFs), which are transcription factors, physiologically induced when the cell is exposed to hypoxia. However, in a pseudohypoxic state, the HIF pathways are constitutively active, independently of oxygen cellular levels (Gruber and Simon, 2006; Dahia, 2014; Gunawardane and Grossman, 2017; Jochmanova and Pacak, 2018).

Physiologically, HIFs are heterodimeric complexes composed by α- and β-subunits (Gruber and Simon, 2006). HIF-α family members include HIF-1α, HIF-2α and HIF-3α, which are the three isoforms of the α-subunit. HIF-β also has three isoforms: ARNT, ARNT2 and MOP3 (member of PAS protein 3) (Gruber and Simon, 2006; Jochmanova et al., 2013). While HIF-β is constitutively expressed in the nucleus, the HIF-α protein expression is related to oxygen levels, therefore regulating HIF activity. In normoxia, HIF's activity is regulated by prolyl-hydroxylase domain enzymes (PHDs), which hydroxylate HIF-α subunits on specific prolyl residues (Gruber and Simon, 2006). This forms a recognition site for von Hippel-Lindau tumor suppressor protein (pVHL), a member of the E3 ubiquitin ligase complex. That complex induces polyubiquitylation of the α-subunits, leading therefore to their proteasomal degradation (the ubiquitin-proteasome pathway) (Gruber and Simon, 2006; Jochmanova et al., 2013) (Figure 3). In hypoxia, the proteasomal degradation is inhibited because the hydroxylation of HIFs, referred above, does not occur (Gruber and Simon, 2006). HIF-α will form a heterodimeric complex with HIF-β, binding to the hypoxia responsive elements (HRE) in the target genes, activating their transcription. Genes coding growth factors like VEGF, PDGF and TGFα, and metabolic enzymes like GLUT1 are examples of the target genes referred above. This will allow the adaptation of cells to a hypoxic state, inducing glycolysis as an alternative to oxidative phosphorylation and angiogenesis, two features relevant for tumorigenesis (Gottlieb and Tomlinson, 2005; Jochmanova et al., 2013).

Loss-of-function mutations in *SDHx, SDHAF2, FH* and *MDH2* leads to the accumulation of Krebs cycle metabolites (succinate, fumarate and malate). More specifically, *SDHx* and *SDHAF2* inactivating mutations lead to an accumulation of succinate, because it's not converted into fumarate on the Krebs cycle. The accumulated succinate goes to cytosol, where it inhibits the PHDs, leading to the stabilization of HIF and consequent activation of target genes – a cellular state known as pseudohypoxia (Jochmanova et al., 2013). Fumarate accumulation, resulting from *FH* mutations, also inhibits PHDs and consequently leading to HIF-α stabilization (Isaacs et al., 2005). Mutations in *MDH2* gene (MDH2 converts malate into oxaloacetate, in the Krebs cycle) are probably associated with fumarate accumulation, however, the mechanism is not completely understood (Cascon et al., 2015). In tumors presenting mutations in genes like *VHL, EGLN1/2* and *HIF2A*, the HIF signaling pathway is activated because they are directly involved in hypoxic signaling (Jochmanova and Pacak, 2018). *VHL* codes for the VHL protein, a member of the E3 ubiquitin ligase complex, *EGLN1* and *EGLN2* code for PHD2 and PHD1 enzymes, respectively and *HIF2A* codes for the subunit 2α of HIF. Tumors included in this cluster typically have a poor prognosis, being more clinically aggressive and often metastatic (Jochmanova and Pacak, 2018).

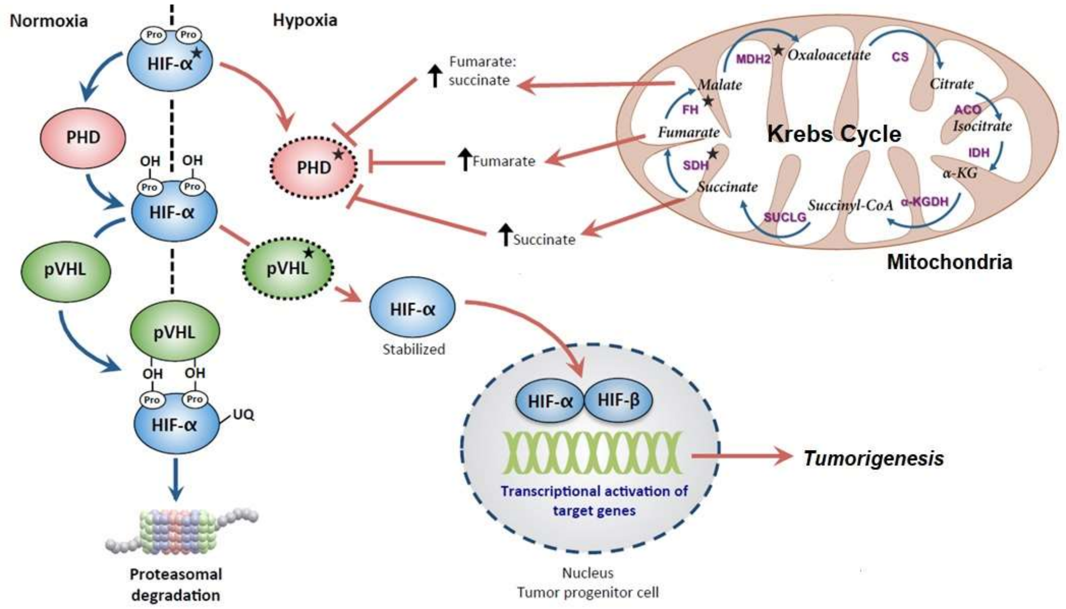
Normoxia
Hypoxia
Pro
Pro
HIF-α
PHD
OH
OH
HIF-α
pVHL
pVHL
OH
OH
HIF-α
UQ
Proteasomal degradation
PHD
pVHL
HIF-α
Stabilized
Fumarate: succinate
Fumarate
Succinate
MDH2
Oxaloacetate
CS
Citrate
Malate
FH
ACO
Isocitrate
Fumarate
Krebs Cycle
IDH
α-KG
SDH
Succinate
SUCLG
Succinyl-CoA
α-KGDH
Mitochondria
HIF-α
HIF-β
Transcriptional activation of target genes
Nucleus
Tumor progenitor cell
Tumorigenesis

Figure 3 - Normoxia cellular state with hypoxia pathway inhibition and consequent proteasomal degradation of HIFs (on the left). Hypoxia or pseudoxypoxia cellular state with activation of the hypoxia pathway, stabilization of HIFs and consequent transcription of target genes, promoting tumorigenesis (on the right). Adapted from Gupta et al. (2017).

6.2 Kinase Signaling Cluster

The tumors included in this group typically harbor somatic and germline mutations in *RET*, *NF1*, *MAX* and *TMEM127* genes, which are related with kinase signaling (Dahia, 2014).

The physiological activation of RET, a transmembrane tyrosine kinase receptor coded by *RET* proto-oncogene, initiates a cascade of events activating RAS and PI3K/AKT downstream signals, including mTOR that regulates cell growth related processes (Dahia, 2014; Pang et al., 2019). Gain-of-function mutations in *RET* gene will result in the constitutive activation of the transmembrane tyrosine kinase receptor, leading to tumorigenesis (Dahia, 2014; Pang et al., 2019).

NF1, which acts as a tumor suppressor gene, codes for neurofibromin, which is a GTPase-activating protein that negatively regulates RAS signaling (Dahia, 2014; Pang et al., 2019). The decreased activity of neurofibromin, caused by loss-of-function mutations in *NF1*, leads to an uncontrolled activation of the RAS signaling, increasing tumorigenesis processes (Pang et al., 2019).

TMEM127 acts as a tumor suppressor gene and encodes TMEM127 protein. The decreased activity of TMEM127 protein, by loss-of-function mutations, allows the activation of the mTOR pathway, independently of RAS and PI3K/AKT (Qin et al., 2010; Gunawardane and Grossman, 2017).

MAX gene encodes a transcriptional regulator, MAX, which can form heterodimers with transcription factors MYC (oncogenic proprieties) and MXD1 (MYC repressor), controlling (inhibiting or promoting) the transcription of genes involved with cellular proliferation, differentiation and apoptosis (Comino-Mendez et al., 2011; Pang et al., 2019). The balanced activity between MYC-MAX and MXD1-MAX heterodimers is essential for the MAX-mediated transcriptional control referred above (Dahia, 2014) (Figure 4).

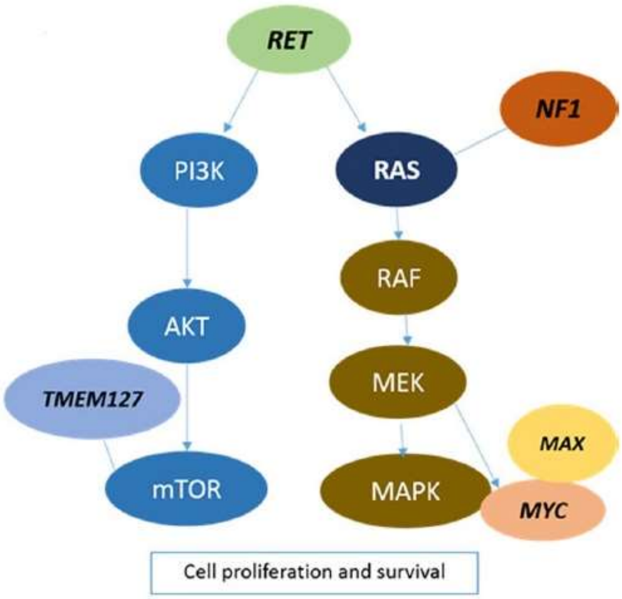

Figure 4 - Schematic representation of the kinase signaling cluster genes and signaling pathways. Adapted from Katabathina et al. (2019).

6.3 Wnt Signaling Cluster

The tumors included in this group are associated with *CSDE1* somatic mutations or fusion genes involving *MAML3,* such as *UBTF-MAML3* and *TCF4-MAML3* (Jochmanova and Pacak, 2018)*.* Alterations in these genes appeared to be two independent ways for Wnt and Hedgehog signaling pathways activation (Fishbein et al., 2017; Gunawardane and Grossman, 2017). The Wnt (or β-catenin) pathway is known for regulating cell proliferation, adhesion, polarity, motility and differentiation. One target gene of this pathway is the oncogene *MYC,* known as a driver of cell proliferation (Bielinska et al., 2009). Typically, the tumors included in this cluster are sporadic pheochromocytomas, with a poor prognosis (Fishbein et al., 2017; Jochmanova and Pacak, 2018).

7. Hereditary Pheochromocytoma and Paraganglioma (HPPGL)

Although the majority of the PPGLs are considered sporadic, about 40% of the cases are associated with germline mutations, being therefore considered hereditary (Dahia, 2014; Castro-Vega et al., 2016; Lam, 2017; Fishbein, 2019). Indeed, PPGLs are considered the most strongly hereditary group of tumors among human cancers (Dahia, 2014; Castro-Vega et al., 2016; Lam, 2017).

PPGLs have a highly diverse genetic background, including germline pathogenic variants in *VHL* (Crossey et al., 1994), *NF1* (Xu et al., 1992), *RET* (Mulligan et al., 1993), *SDHA* (Burnichon et al., 2010), *SDHB* (Astuti et al., 2001), *SDHC* (Niemann and Muller, 2000), *SDHD* (Baysal et al., 2000) , *SDHAF2/SDH5* (Hao et al., 2009), *TMEM127* (Qin et al., 2010), *MAX* (Comino-Mendez et al., 2011), *EGLN1/PHD2* (Ladroue et al., 2008), *KIF1B* (Yeh et al., 2008), *EPAS1/HIF2A* (Lorenzo et al., 2013), *FH* (Castro-Vega et al., 2014), *MEN1* (Dackiw et al., 1999), *MDH2* (Cascon et al., 2015), *EGLN2/PHD1* (Yang et al., 2015), *KMT2D* (Juhlin et al., 2015) and *BAP1* (Wadt et al., 2012) genes (Table 1). For several of these genes, germline mutations cause hereditary tumor syndromes, in which PHEOs and/or PGLs can be one of the clinical manifestations. Germline mutations in *SDHx* and *SDHAF2* are the most common genetic cause of inherited PPGLs (Lam, 2017).

The likelihood of finding a germline pathogenic variant in a patient with a PHEO or a PGL increases when one, or more, of the following features is present: young age at presentation (less than 45 years old); associated syndromic manifestations; multifocal, bilateral, or metastatic disease; and/or a positive family history (based on family pedigree or identification of susceptibility gene mutation in a relative) (Cascon et al., 2009; Mannelli et al., 2009; Buffet et al., 2012). However, the presence of those characteristics is not mandatory (Lenders et al., 2014). The diagnosis of a HPPGL is established when a germline heterozygous pathogenic variant is found in the proband (Else et al., 2018).

Table 1 - Genes associated with HPPGL, chromosomal locus, associated syndrome, germline pathogenic variants prevalence and mode of inheritance. Adapted from Muth et al. (2019).

Gene	Locus	PPGL syndrome	Prevalence	Mode of inheritance
RET	10q11.21	MEN2	5%	AD
VHL	3p25.3	VHL	13%	AD
NF1	17q11.2	NF1	3%	AD
MEN1	11q13.1	MEN1	< 1%	AD
FH	1q43	HLRCC	1%	AD
SDHA	5p15.33	PGL5	1%	AD
SDHB	1p36.13	PGL4	8-10%	AD
SDHC	1q23.3	PGL3	2%	AD
SDHD	11q23.1	PGL1	7-10%	AD [a]
SDHAF2	11q12.2	PGL2	1%	AD [a]
TMEM127	2q11.2	-	1-2%	AD
MAX	14q23.3	-	1%	AD
KIF1B	1p36	-	*	AD
PHD2/EGLN1	1q42.2	-	*	AD
PHD1/EGLN2	19q13.2	-	*	AD
EPAS1/HIF2A	2p21	-	*	AD
MDH2	7q11.23	-	*	AD
KMT2D	12q13.12	-	*	AD
BAP1	3p21.1	-	*	AD

*not available; [a] Autosomal dominant with "parent-of-origin" expression phenotype.

7.1 Syndromic Forms

Germline mutations in *RET, VHL, NF1, MEN1* and *FH* genes are related with the following hereditary syndromes: MEN2 (Multiple Endocrine Neoplasia type 2A and 2B), VHL (von Hippel-Lindau disease), NF1 (Neurofibromatosis type 1), MEN1 (Multiple Endocrine Neoplasia type 1) and HLRCC (Hereditary Leiomyomatosis and Renal Cell Carcinoma syndrome), respectively. All of these are well-established hereditary syndromes, in which PHEOs (more commonly) and/or PGLs, are one of the clinical manifestations (Lam, 2017). The diagnosis of these five syndromes can be performed based on clinical criteria and they are also characterized by the presence of syndromic lesions (involving organs other than the adrenals or the paraganglia) (Mannelli et al., 2009; Else et al., 2018; Muth et al., 2019). The mode of inheritance is autosomal dominant and germline mutations are present in about 23% of all HPPGL cases. *VHL* germline mutations are the most prevalent, representing about 13% all HPPGL cases, followed by *RET* (≈5%) and *NF1* (3%) genes. The occurrence of PPGL in MEN1 and HLRCC syndromes is much rarer, with only a small percentage (≈1%) of cases presenting germline mutations in *MEN1* and *FH* genes (Muth et al., 2019).

7.1.1 Multiple Endocrine Neoplasia type 2

Multiple Endocrine Neoplasia type 2 (MEN2) is an autosomal dominant syndrome caused by germline activating mutations in the *RET* proto-oncogene (Wohllk et al., 2010). This gene is located on chromosome 10q11.2, has 21 exons and encodes an 860 amino acid protein, which is a transmembrane receptor tyrosine kinase (Lodish and Stratakis, 2008). Clinical diagnostic criteria are medullary thyroid carcinoma (MTC), PHEO and primary hyperparathyroidism (Fishbein, 2019).

There are three subtypes of MEN2 associated with *RET* mutations: MEN2A, MEN2B and familial medullary thyroid carcinoma (FMTC). The MEN2A subtype represents the majority of cases (90%) and the mutational spectrum related to this subtype includes missense mutations in exon 10 (codons 609, 610, 611, 618, 620) and exon 11 (codon 634) (Brandi et al., 2001; Fishbein and Nathanson, 2012). These mutations occur in the extracellular domain of RET, causing activation of PI3 kinase pathway in a ligand independent manner. That activation leads to a higher capacity of the cell to grow, differentiate and survive (Wohllk et al., 2010). The MEN2B subtype is much less common (5% of the cases) and mostly associated with mutations at exon 16 (codon 918) (Pacak et al., 2009; Wohllk et al., 2010). Lastly, the FMTC subtype is the rarest subtype, and it’s characterized by the absence of PHEO. The mutational spectrum of these patients includes mutations in exon 10, 11 and 13 (codon 768) and exon 14 (codons 804, 806) (Brandi et al., 2001).

The identification of a PHEO in a patient with MEN2 syndrome is clinically relevant because prevention of a possible hypertensive crisis during a surgical treatment becomes possible (Gunawardane and Grossman, 2017). About 50% of MEN2 syndrome patients will develop PHEO, and approximately half of them will present bilateral disease (Fishbein, 2019).

7.1.2 von Hippel-Lindau disease

The VHL disease is a rare autosomal dominant syndrome caused by germline mutations on *VHL* tumor suppressor gene (Latif et al., 1993). This gene is located on chromosome 3p25.3, contains three exons and encodes two proteins: $pVHL_{30}$ and $pVHL_{19}$. These proteins are involved in HIF1α and HIF2α proteasomal-mediated degradation and ubiquination, regulating the transcription of hypoxia inducible genes (Latif et al., 1993). VHL disease is characterized by either benign and malignant tumors, including CNS hemangioblastomas, clear cell renal cell carcinoma (RCC), pancreatic neuroendocrine tumors, renal, pancreatic and epididymal cysts and PHEOs. VHL disease can be divided into type 1 and type 2, based on the likelihood of developing PHEO, with type 2 families presenting an increased risk (Gunawardane and Grossman, 2017). Above 10 to 20% of patients develop benign and bilateral PHEOs, and it can be one of the first clinical manifestations of the syndrome (Delman et al., 2006; Fishbein and Nathanson, 2012). Although rare, there are reports of sympathetic and parasympathetic PGLs in these patients (Boedeker et al., 2009). The age of diagnosis of PPGL in VHL syndrome is about 28 years, and they are generally bilateral, multiple and asymptomatic at diagnosis (Maher et al., 2011; Jafri and Maher, 2012). The most common *VHL* gene mutations are deletions, truncating and splice-site, being associated with a lower risk for PPGLs development. However, missense mutations are associated with a higher risk for PHEO development (Jafri and Maher, 2012; Fishbein, 2019).

7.1.3 Neurofibromatosis type 1

NF1 is an autosomal dominant genetic disorder caused by germline mutations on the tumor suppressor gene *NF1* (Fishbein and Nathanson, 2012). *NF1* is located on chromosome 17q11.2, contains sixty exons and has multiple pseudogenes (Fishbein and Nathanson, 2012; Gunawardane and Grossman, 2017; Pang et al., 2019). Up to 50% of NF1 syndrome patients have a *de novo* mutation, with variable penetrance and disease expressivity, even in patients with the same mutation (Ferner et al., 2007) which makes it difficult to establish a relationship between genotype and phenotype. A wide variety of germline mutations have been described, namely points mutations, which include nonsense, missense, insertion/deletions, and splicing mutations, and large genomic rearrangements (Shen et al., 1996; Fokkema et al., 2011).

NF1 diagnosis is mostly clinical and requires the presence of at least two or more of the following clinical features: *café-au-lait* macules, neurofibromas, optic glioma, Lisch nodules, bony dysplasia, axillary and inguinal freckling and a first degree relative with the disease (Ferner et al., 2007). Although, the occurrence of PHEO is not a criterion for NF1 syndrome diagnosis, they occur in approximately 3 % of all NF1 patients (L. M. Gruber et al., 2017; Fishbein, 2019).

7.1.4 Multiple Endocrine Neoplasia type 1

MEN1 is an autosomal dominant genetic disorder caused by germline mutations in the tumor suppressor gene *MEN1* (Marini et al., 2006). This gene is located on chromosome 11q13.1, contains ten exons and encodes menin, a 610 amino acid protein. Menin has a nuclear localization, probably suggesting an important role in the regulation of DNA transcription and replication, in cell cycle and genome integrity maintenance (Marini et al., 2006). Clinically, MEN1 is characterized by the presence of hyperplasia and neoplasia in at least two endocrine tissues (parathyroid adenomas, entero-pancreatic and pituitary tumors). PHEO is a very rare clinical manifestation of MEN1, occurring in less than 1% of the patients (Dackiw et al., 1999).

7.1.5 Hereditary Leiomyomatosis and Renal Cell Carcinoma syndrome

HLRRC syndrome is an autosomal dominant syndrome caused by germline mutations in the tumor suppressor gene *FH*, which is located on chromosome 1q42.1, has eight exons and encodes fumarase (Favier et al., 2015). This enzyme is part of the Krebs cycle, converting fumarate to malate. This syndrome is characterized by the occurrence of smooth muscle tumors (leiomyomas) in the skin and uterus, and type 2 papillary renal cell carcinoma. PPGLs are an exceptional manifestation of the disease, occurring in less than 1% of the patients (Castro-Vega et al., 2014; Favier et al., 2015).

7.2 Other Susceptibility Genes Described for Hereditary PPGL

Germline pathogenic variants in *TMEM127* (2q11.2), *MAX* (14q23.3), *KIF1B* (1p36), *EGLN1/PHD2* (1q42.2), *EPAS1/HIF2A* (2p21), *MDH2* (7q11.23), *EGLN2/PHD1* (19q13.2), *KMT2D* (12q13.12) and *BAP1* (3p21.1) are much less frequent, when compared to the previously referred genes.

TMEM127 germline mutations have been associated with PHEO susceptibility, are present in 1-2% of inherited cases, and the mutational spectrum includes frameshift, in-frame deletions, missense and nonsense variants (Fokkema et al., 2011; Muth et al., 2019).

MAX mutations have also been associated with PHEO susceptibility and germline mutations are present in about 1% of the cases. The mutational spectrum mainly includes missense, nonsense and frameshift variants (Fokkema et al., 2011; Muth et al., 2019) (Comino-Mendez et al., 2011; Gunawardane and Grossman, 2017).

Regarding the remaining genes, germline mutations have only been reported in rare or single cases, and their role in the etiology of PPGL remains unclear (Yeh et al., 2008; Wadt et al., 2012; Lorenzo et al., 2013; Buffet et al., 2014; Cascon et al., 2015; Juhlin et al., 2015; Yang et al., 2015).

7.3 Hereditary PPGL Related to *SDHx*

SDHA, SDHB, SDHC, SDHD and *SDHAF2* are the genes that code for the four subunits and the cofactor of the succinate dehydrogenase (SDH) mitochondrial enzyme. This enzyme, also known as succinate-ubiquinone oxidoreductase, is a highly conserved heterotetrametric mitochondrial protein (Bardella et al., 2011). SDHA and SDHB are the catalytic subunits, which protrude into the mitochondrial matrix and are anchored to the inner membrane by SDHC and SDHD subunits, which also provide the binding site for ubiquinone (Bardella et al., 2011) (Figure 5). SDH forms the mitochondrial complex II and is the only mitochondrial enzyme that participates both in the Krebs cycle and in the electron transport chain (ETC). In the Krebs cycle, SDH performs the oxidation of succinate to fumarate and, in the ETC, SDH participates in the electron transfer to the terminal acceptor ubiquinone (ubiquinone reduction) (Gottlieb and Tomlinson, 2005; Bardella et al., 2011; Aldera and Govender, 2018). The Krebs cycle links the glucose metabolism in the cytosol and the oxidative phosphorylation in the mitochondria (Gottlieb and Tomlinson, 2005).

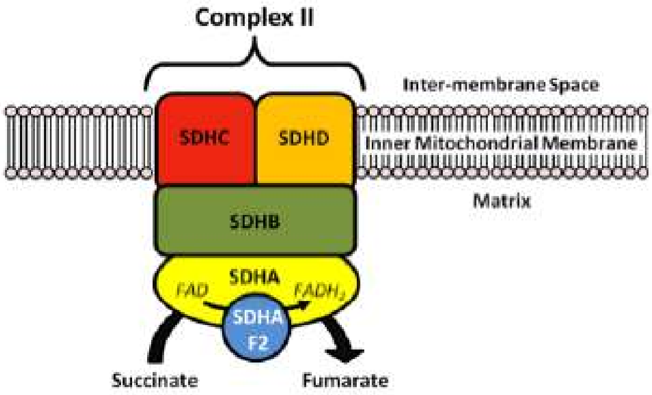

Figure 5 - Illustration of the mitochondrial succinate dehydrogenase enzyme (or complex II of the electron transport chain), including the four subunits (SDHA, B, C, D) and the SDHAF2 cofactor. Adapted from Ricketts et al. (2012).

HPPGLs syndromes caused by mutations in the *SDHx* and *SDHAF2* genes can be classified in five groups: PGL type 1, PGL type 2, PGL type 3, PGL type 4 and PGL type 5, according to the presence of germline mutations in the *SDHD*, *SDHAF2*, *SDHC*, *SDHB* and *SDHA* genes, respectively (Benn et al., 2015). All of these HPPGL types present an autosomal dominant inheritance, however, regarding *SDHD* and *SDHAF2* the disease only occurs when associated with paternally inherited pathogenic variants (Bayley et al., 2014; Else et al., 2018). Generally, PGLs are more frequently diagnosed than PHEOs in patients with *SDHx* mutations (Benn et al., 2015). Beyond PPGLs, other types of tumors characterize these syndromes like RCC, gastrointestinal stromal tumors (GISTs) and pituitary adenomas (PA), with a variable risk of development (Benn et al., 2015). Patients with PGL type 4 and 1 present a risk for RCC of approximately 14% and 8%, respectively (Gill et al., 2011; Benn et al., 2015). The risk for developing GISTs is higher for patients with PGL type 5, but they also have been described in patients with PGL types 1, 3 and 4 (Benn et al., 2015; Boikos et al., 2016). PA is a very rare clinical manifestation that has been described in some case reports (Gill et al., 2014).

7.3.1 Hereditary PPGL related to *SDHD* (PGL type 1)

PGL type 1 is mainly associated with bilateral or multifocal head-and-neck PGLs, however, unilateral PHEOs and sympathetic PGLs have also been reported (Gunawardane and Grossman, 2017). Although metastatic disease is uncommon, occurring in less than 5% of the patients (Ricketts et al., 2010), the reported lifetime penetrance is considered high, given that at the age of 40 about 75% of the paternally inherited mutations carriers manifest the disease (Benn et al., 2006). Mean ages at diagnosis of head-and-neck PGLs and PHEOs are approximately 40 and 20 years of age, respectively (Ricketts et al., 2010). The *SDHD* gene, located at 11q23.1, has four exons and encodes a 103 amino acid protein, the D subunit of the SDH enzyme (Baysal et al., 2000). According to the LOVD database, the mutational spectrum of *SDHD* includes frameshift, in frame deletions, indels, missense and nonsense variants and large genomic rearrangements (Fokkema et al., 2011).

7.3.2 Hereditary PPGL related to *SDHAF2* (PGL type 2)

PGL type 2 has been identified in a small number of PPGL patients, so mutations in the *SDHAF2* gene are a rare cause of inherited disease. Clinically, head-and-neck PGLs are the typical manifestation, and the mean age at diagnosis is 30 years old (Gunawardane and Grossman, 2017). The tumors are often multifocal and about 75% of the paternally inherited mutation-carriers will develop head-and-neck PGLs (Benn et al., 2015). The

SDHAF2 gene, located at 11q12.2, has four exons and encodes a 166 amino acid protein, which is a SDH enzyme cofactor, essential for the flavination of the SDHA subunit (Fishbein and Nathanson, 2012). According to the LOVD database, the mutational spectrum of *SDHAF2* includes mainly missense variants, with only one frameshift alteration reported (Fokkema et al., 2011).

7.3.3 Hereditary PPGL related to *SDHC* (PGL type 3)

PGL type 3 is mainly associated with head-and-neck (more specifically, carotid body) PGLs, being PHEOs and extra-adrenal PGL less common. Mutations in *SDHC* are a rare cause of hereditary PPGL, being present in only about 4% of head-and-neck PGLs, and the risk of metastatic disease is low (Schiavi et al., 2005; Fishbein and Nathanson, 2012). The *SDHC* gene located at 1q23.3, has six exons, and encodes a 169 amino acid protein, the succinate dehydrogenase complex subunit C. According to the LOVD database, the mutational spectrum includes missense, frameshift, nonsense, in-frame deletion and duplication variants and large genomic rearrangements (Fokkema et al., 2011).

7.3.4 Hereditary PPGL related to *SDHB* (PGL type 4)

PGL type 4 is clinically characterized by the occurrence of unifocal disease and extra-adrenal sympathetic PGLs, which are more frequently diagnosed than PHEOs and parasympathetic PGLs (Timmers et al., 2007; Jochmanova et al., 2017).

The *SDHB* gene, located at 1p36.13, has eight exons and encodes a 280 amino acid protein, which is the B subunit (or iron-sulfur subunit) of the SDH enzyme. Patients with mutations in the *SDHB* gene present more frequently metastatic disease (Jochmanova et al., 2017; Andrews et al., 2018), so every patient diagnosed with a PPGL should be tested for *SDHB* mutations (Amar et al., 2007; R. Martins and Bugalho, 2014; Lam, 2017). According to the LOVD database, the mutational spectrum of *SDHB* comprises missense, nonsense, frameshift, in frame duplications or deletions and large genomic rearrangements (Fokkema et al., 2011).

7.3.5 Hereditary PPGL related to *SDHA* (PGL type 5)

PGL type 5 is a rare cause of sympathetic and parasympathetic PGLs, with less than 1% of the cases harboring *SDHA* germline mutations (Toledo et al., 2017). The *SDHA* gene, located at 5p15.33, contains 15 exons and encodes a 621 amino acid protein, being therefore the largest gene of the *SDH* group of genes (Benn et al., 2015). According to the

LOVD database, the mutational spectrum of *SDHA* includes missense, nonsense, frameshift and in frame deletions (Fokkema et al., 2011). *SDHA* gene has three pseudogenes, *SDHAP1* (3q29), *SDHAP2* (3q29) and *SDHAP3* (5p15.33). These pseudogenes are highly homologous with *SDHA* intronic and coding regions, complicating the genetic analysis of this gene (Benn et al., 2015; Fishbein, 2019).

7.4 *SDHB* Exon 1 Deletion

The mutational spectrum of the *SDHB* gene mainly includes missense and nonsense mutations, nonetheless a significant amount of HPPGL patients present large genomic rearrangements (Fokkema et al., 2011). Several large deletions have been reported in HPPGL families from many different countries and some of them are associated with founder effects (Bayley et al., 2009; Hensen et al., 2012; Rijken et al., 2016). The *SDHB* exon 1 deletion has been reported recurrently in several countries, but in the majority of them the genomic breakpoints were not determined (Table 2). Given the high frequency of large deletions involving *SDHB* exon 1, this region can be a possible hot spot for gross deletions within the *SDHB* gene (Cascon et al., 2006). The intron 1 region of *SDHB* presents a high density of *Alu* repeats, which are thought to be involved in chromosomal rearrangements and homologous recombination events (Cascon et al., 2006; Hoekstra et al., 2017). Therefore, Alu-mediated recombination has been proposed as a possible mechanism responsible for these rearrangements (Cascon et al., 2006; Hoekstra et al., 2017).

Particularly, one *SDHB* exon 1 deletion has been described as a founder mutation in the Iberian Peninsula (Cascon et al., 2008; Martins et al., 2013). The first description of this rearrangement was made in a Brazilian family, in a study that searched for large genomic rearrangements in patients that tested negative for point mutations in known PPGLs susceptibility genes (McWhinney et al., 2004). Subsequently, additional families were reported to present this *SDHB* exon 1 deletion, namely three Spanish and one Portuguese families (Cascon et al., 2008). Genomic breakpoint characterization revealed that all these families presented the same 15,678 bp deletion (Cascon et al., 2008). Furthermore, all these families were originated from the northwest of the Iberian Peninsula and shared a common haplotype, suggesting a founder effect (Cascon et al., 2008). This rearrangement was also observed in a large family with Mexican-Spanish origin (Solis et al., 2009). More recently, Martins et al (2013) reported 11 families from the north of Portugal with this rearrangement (Martins et al., 2013). Haplotype analysis, using SNPs, revealed a conserved region in all the patients harboring this deletion, suggesting a founder effect (Cascon et al., 2008; Martins et al., 2013).

Table 2 - Gross deletions involving *SDHB* exon 1 described in the literature until August 2019.

***SDHB* Rearrangement**	**Breakpoint characterized**	**Country**	**Nº of cases**	**Authors**
Iberian *15,678 bp* deletion	Yes	Brazil	1	(McWhinney et al., 2004)
Iberian *15,678 bp* deletion	Yes	Spain and Portugal	2	(Cascon et al., 2006)
c.1-?_72+?del	No	France	2	(Amar et al., 2007)
Iberian *15,678 bp* deletion	Yes	Brazil, Spain and Portugal	5*	(Cascon et al., 2008)
Exon 1 deletion	No	European-American Paraganglioma Registry	2	(Neumann et al., 2009)
Iberian *15,678 bp* deletion	Yes	Mexico	1	(Solis et al., 2009)
Exon 1 deletion	No	USA	2	(Lodish et al., 2010)
c.1-16416_72-3886del	Yes	France	1	(Buffet et al., 2012)
c.1-10413_73-3867del	Yes	France	1	(Buffet et al., 2012)
c.1-?_72-?del	No	France	1	(Buffet et al., 2012)
Exon 1 deletion	No	USA	3	(Ricketts et al., 2012)
Exon 1 deletion	No	Switzerland	1	(Weber et al., 2012)
Exon 1 deletion	No	France	2	(Lefebvre et al., 2012)
Iberian *15,678 bp* deletion	Yes	Portugal	11	(Martins et al., 2013)
Exon 1 deletion	No	United Kingdom	1	(Rattenberry et al., 2013)
Exon 1 deletion	No	United Kingdom	1	(Cilliers et al., 2013)
Exon 1 deletion	No	Brazil	3	(Moraes, 2014)
Exon 1 deletion	No	United Kingdom	1	(Fowler et al., 2016)
Exon 1 deletion	No	Poland	1	(Michalowska et al., 2016)
Exon 1 deletion	No	Denmark	1	(Bennedbaek et al., 2016)
Exon 1 deletion	No	United Kingdom	1	(Parrish et al., 2017)
Exon 1 deletion	No	United Kingdom	17	(Andrews et al., 2018)
c.(?_1-173)_(1-87_109) del	No	Portugal	8	(Donato et al., 2019)
Exon 1 deletion	No	Spain	1	(Guerrero-Perez et al., 2019)
Exon 1 deletion	No	United Kingdom	5	(Tufton et al., 2019)

* Five cases include two new Spanish cases and also the three cases already reported by Cascon et al., (2006) and McWhinney et al., (2004).

II. AIMS

II. Aims

This study aimed to characterize, at a national level, patients with hereditary paraganglioma-pheochromocytoma carrying a frequent *SDHB* exon 1 deletion.

Specifically, the aims of this project were:

- To characterize the genomic breakpoint in the patients with a *SDHB* exon 1 deletion;
- To perform an extensive haplotype study using closely linked microsatellite markers in carrier families;
- To estimate the age of the *SDHB* exon 1 deletion;
- To gain insight about the geographical distribution of the *SDHB* exon 1 deletion positive families;
- To estimate the penetrance of all clinical manifestations in *SDHB* exon 1 deletion carriers;

III. MATERIALS AND METHODS

III. Materials and Methods

1. Clinical Samples

This study included 30 HPPGL families presenting a *SDHB* exon 1 deletion (*SDHB* c.(?_-151)_(72+1_73-1)del, HGVS, LRG_316t1) previously detected by Multiplex Ligation Probe Amplification (MLPA). Twenty-four families were studied by routine genetic diagnosis, during the period of 2010 to 2019, at the Genetics Department of the Portuguese Oncology Institute of Porto. Eleven of these 24 families had been previously studied in the context of a research project developed in IPATIMUP (Martins et al., 2013). Additionally, four and two families were identified by routine genetic diagnosis at the Portuguese Oncology Institute of Lisbon and Coimbra, respectively. Additionally, 106 family members, including 77 carriers, were also studied.

After genetic counseling and informed consent, DNA was isolated from peripheral blood samples using Magna Pure LC 2.0 [Roche Applied Science, Indianapolis, Indiana] according to the manufacturer’s instructions and the DNA quality and concentration were evaluated using a NanoDrop ND-1000® [NanoDrop Technologies, Wilmington, DE, USA]. All the samples were screened for large genomic rearrangements by MLPA, using the SALSA MLPA P226 SDH Kit [MRC-Holland, Amsterdam, Netherlands], according to the manufacturer´s protocol.

The geographic origin of the families presenting the *SDHB* exon 1 deletion was inferred from the birthplace of the oldest carrier or of the oldest affected family member most likely to be a carrier.

2. *SDHB* Exon 1 Germline Deletion Breakpoint Identification

To characterize the deletion breakpoints of the *SDHB* exon 1 germline deletion, a PCR specific amplification and Sanger sequencing were performed, using primers that flanked the 15,678 bp deletion previously described as an Iberian Peninsula founder deletion (Solis et al., 2009).

For this purpose, approximately 20 ng of DNA were amplified in a solution containing 1x Taq reaction buffer (75 mM Tris-HCl, 20 mM $(NH_4)_2SO_4$) [Thermo Fisher Scientific, Waltham, USA], 2 mM of $MgCl_2$ [Thermo Fisher Scientific], 0,5 mM dNTP mix [Thermo Fisher Scientific], 1 U of Taq DNA polymerase [Thermo Fisher Scientific], 0.15 µM of SDHB exon 1 Del F: 5’-GTAAAATAGATACGAGCCATCACTGG-3’ and 0.15 µM of SDHB exon 1 Del R: 5’-TAGTAGGGTAAGTGGGACAATATGCC-3’ [Metabion, Germany], and bidistilled sterile water [B. Braun Medical Lda, Portugal] in a final reaction volume of 20 µL. PCR reaction was performed in a thermocycler [Biometra, Analytik Jena, Germany] according to the conditions indicated in Table 3. Amplified PCR products were analyzed by electrophoresis in a 2% (w/v) agarose gel [Thermo Fisher Scientific] stained with GreenSafe [Nzytech, Lisbon, Portugal] 0.05 µL/mL. The amplification of a 228 bp fragment indicates the presence of the 15678 bp Iberian Peninsula founder deletion.

Table 3 - PCR program used for the detection of the *SDHB* exon 1 deletion.

Temperature	**Time**	
95ºC	10 minutes	
95ºC	45 seconds	35 cycles
58ºC	45 seconds	
72ºC	45 seconds	
72ºC	10 minutes	
4ºC	Pause	

Amplified PCR products were purified using the ExoSAP-IT method, for the removal of primers and dNTPs in excess. Samples were purified adding 2 µL of ExoSAP solution (Exonuclease I [Thermo Fisher Scientific] (20 U/µL) and Fast Thermosensitive Alkaline Phosphatase [Thermo Fisher Scientific] (1 U/µL), in a proportion of 1:2) to 5 µL of the PCR product, followed by incubation at 37ºC for 50 minutes, and enzyme inactivation at 85ºC for 15 minutes.

Sanger sequencing was performed using BigDye™ Terminator v3.1 [Thermo Fisher Scientific] following the manufacturer´s instructions. The reaction was performed using 3.4 µL of BigDye™ Terminator 5x sequencing buffer, 0.5 µL of Big Dye™ Terminator v3.1, (containing dNTPs, ddNTPs-fluorocromes, $MgCl_2$ and Tris-HCl buffer), 0.32 µL of a 10 µM primer solution, 1 µL of the previously purified DNA and bidistilled sterile water [B. Braun Medical Lda] to reach a final reaction volume of 10 µL The sequencing reaction was performed using the conditions presented in Table 4.

Table 4 - PCR program used for the sequencing reaction.

Temperature	Time	
95ºC	4 minutes	
95ºC	10 seconds	35 cycles
50ºC	10 seconds	
60ºC	2 minutes	
60ºC	10 minutes	
4ºC	Pause	

The sequencing products were purified with Illustra Sephadex® G-50 fine [GE Healthcare, Life Sciences, Chicago, USA], according to standard procedures, for the removal of the excess dNTPs, labeled ddNTPs and non-incorporated primers. Then, 15 µL of Hi-Di^{TM} Formamide [Thermo Fisher Scientific] were added to the previously purified products, in order to help the stabilization of the single stranded DNA. Sequencing analysis was performed by capillary electrophoresis on a 3500 Genetic Analyser [Thermo Fisher Scientific]. Electropherograms were analysed by the Sequencing Analysis Software v6 [Thermo Fisher Scientific] and sequences were manually reviewed at least twice.

3. *SDHB* Exon 1 Deletion Specific Assay

After breakpoint identification, a PCR amplification specific assay was designed to detect the *SDHB* exon 1 rearrangement. This assay consisted of a three-primer PCR selective amplification in which the mutated allele is amplified with primers SDHB EX1del BKP F: 5´-TGTGGAAATAGGCACATTCCTTAAA-3´ (forward) and SDHB EX1del BKP MUT R: 5´-AAATGGGGCTACTTCAAGTTTTTACT-3´ (reverse), and the normal allele with the same forward primer and the reverse primer SDHB EX1del BKP WT R: 5´-CCTGGGACTCCAAGTACACATTTT-3´ (reverse). This assay was performed in all positive cases and in 27 negative cases.

PCR reactions were performed in a 20 µL reaction containing 20 ng of DNA, 1x Taq reaction buffer (75 mM Tris-HCl, 20 mM $(NH_4)_2SO_4$) [Thermo Fisher Scientific], 2 mM of $MgCl_2$ [Thermo Fisher Scientific], 0,5 mM dNTP mix [Thermo Fisher Scientific], 1 U of Taq DNA polymerase [Thermo Fisher Scientific], 0.15 µM of each primer [Metabion], and bidistilled sterile water [B. Braun Medical Lda]. PCR reaction was performed in a thermocycler [Biometra] according to the conditions indicated in Table 3.

Amplified PCR products were analyzed by electrophoresis in a 2% (w/v) agarose gel [Thermo Fisher Scientific] stained with GreenSafe [Nzytech] 0.05 µL/mL. Amplification of two fragments, one of 351 bp (wild-type allele) and another of 290 bp (mutant allele) indicates that the case is positive for the *SDHB* deletion, whereas in the negative cases only the 351 bp fragment will amplify. Positive cases were confirmed by Sanger sequencing after selective amplification of the mutant allele, using the primers SDHB EX1del BKP F: 5´-TGTGGAAATAGGCACATTCCTTAAA-3´ (forward) and SDHB EX1del BKP MUT R: 5´-AAATGGGGCTACTTCAAGTTTTTACT-3´ (reverse), as described above (Table 4).

The *SDHB* intron 1 breakpoint region of the wild-type allele was also sequenced in all 104 carriers (for three families the DNA from the index case was not available) using primers: SDHB EX1del BKP F 5´- CGGGCAAGGTGGCCTGTA-3´ (forward) and SDHB EX1del BKP WT R: 5´-CCTGGGACTCCAAGTACACATTTT-3´ (reverse) and as described previously. Additionally, this region was also sequenced in 31 non-carrier family members and 50 normal controls (cases without the deletion and unrelated with the HPPGL families).

4. *SDHB* Exon 1 Deletion Genomic Breakpoints and Sequence Context Analysis

Genomic breakpoints were defined as a set of coordinates on the genome spanning the genomic sequence of the deletion and were given using the reference sequence NC_000001.11. The *SDHB* exon 1 deletion nomenclature was described in agreement with the rules recommended by the Human Genome Variations Society guidelines. RepeatMasker software was used to search for low complexity DNA sequences and interspersed repeats in the regions flanking the two breakpoints (upstream *SDHB* 5’ UTR and intron 1 regions).

5. Haplotype Analysis

Haplotype analysis was performed by genotyping microsatellite and single nucleotide polymorphisms (SNPs) markers. Haplotype construction was performed manually and based on probands and their relatives’ genotypes.

5.1 Microsatellite Genotyping

A total of 27 probands and 106 family members were genotyped for polymorphic microsatellite markers flanking the *SDHB* gene, namely D1S507, D1S436, D1S170, D1S2826, D1S2644, D1S2732 and D1S2828. The consensus repeat and the genomic location of the markers are shown in Table 5. The consensus pattern was obtained with the software Tandem Repeats Finder (http://www.tandem.bu.edu/) (Benson, 1999). The genomic location of the microsatellite markers and primer sequences for their amplification were derived from the UCSC Genome Browser (Human GRCh37/hg19 Assembly) (http://genome.ucsc.edu/) (Kent et al., 2002).

Table 5 - Microsatellite markers used for haplotype analysis and respective repeat unit, genomic location and primer sequences.

Microsatellite Marker	Repeat unit	Genomic location	Primer sequence
D1S507	CA	15028720 15028985	F – AGGGGATCTTGGCACTTGG R – CTCTAGGGTTTCTGGAAAATGCTG
D1S436	AC	15870457 15870771	F – TGAATGTGTCTCCAGTGTTAGC R – GTTTCTTCTGTAGAGCAATCTGGCAATATGT
D1S170	AC	17297436 17298256	F – CACTCAGGCAGGTGCATG R – GTTTCTTGAATCTTGTGCATGGTGTGG
D1S2826	CA	18433233 18433591	F – TGGGACTTGTATGTTACCATTACTC R – GTTTCTTCCCTTCATCCTCGCAG
D1S2644	AC	19026467 19026806	F – TGCAACCCACCTGAATGA R – GTTTCTTTACGTGAAGTGCCAGCACA
D1S2732	AC	20309855 20310118	F – TGACTTCAGTGAGGCTGC R – CGGATACAAGGGCTTTTC
D1S2828	AC	21615978 21616249	F – GGCTCCTGAACCTGGG R – AGCTTTGGCTGACCTTCC

All seven markers were assayed by PCR using fluorescently end-labeled primers and fragment analysis. Approximately 20 ng of DNA were amplified in a solution containing 1x Taq reaction buffer (75 mM Tris-HCl, 20 mM $(NH_4)_2SO_4$) [Thermo Fisher Scientific], 2 mM of $MgCl_2$ [Thermo Fisher Scientific], 0,5 mM dNTP mix [Thermo Fisher Scientific], 1 U of Taq DNA polymerase [Thermo Fisher Scientific, Waltham, USA], 0.15 µM of each primer [Metabion, Germany], and bidistilled sterile water [B.

Braun Medical Lda, Portugal]. PCR reaction was performed in a thermocycler [TProfessional Basic 96, Biometra, Analytik Jena, Germany] according to the to the conditions indicated in Table 3. PCR products were analyzed by capillary electrophoresis on a 3500 Genetic Analyzer [Thermo Fisher Scientific, Waltham, USA] after mixing with 20 µL of Hi-Di™ Formamide [Thermo Fisher Scientific, Waltham, USA] and 0.4 µL of fluorescence labeled DNA fragment size standard GeneScan™ 600 LIZ™ [Thermo Fisher Scientific, Waltham, USA]. Allele sizes were determined using the GeneMapper® Software version 5 [Thermo Fisher Scientific, Waltham, USA].

5.2 Haplotype Construction and Estimation of Mutation Age

Haplotype construction was performed manually using the genotypes obtained from probands and family members. The age of the mutation was estimated from the variation accumulated in the ancestral haplotype, as described by Martins et al. (2007). This method considers both recombination (c) and mutation (µ) rates in the generation of variation. The probability of change per generation (ε) is given by $\varepsilon=1-[(1-c)(1-\mu)]$, and the average of mutation and recombination events (λ) equals εt, where t is the number of generations. The recombination rate (c) was estimated from the physical distance between the two most distant markers using a conversion factor calculated in Rutgers Map Interpolator (http://compgen.rutgers.edu/old/map-interpolator/) (Matise et al., 2007). The estimate of average mutation rate used was 7.8×10^{-4} for dinucleotides markers (Gyapay et al., 1994).

5.3 SNPs Markers Genotyping

Haplotype analysis of seven SNPs markers, previously described by Martins et al (2013), flanking the upstream (rs1569754, rs3946080, rs2143811 and rs5772743) and downstream (rs7545518, rs7545499 and rs7536679) regions of the *SDHB* exon 1 deletion was also performed.

SNPs markers genotyping was performed by PCR and Sanger sequencing using the primers indicated in Table 6, and as previously described (Table 3 and Table 4).

Table 6 - Primers used for single nucleotide polymorphisms analysis.

Region	Primers sequence	SNPs
Upstream *SDHB* 5’ UTR	**F –** TGTGGAAATAGGCACATTCCTTAAA **R –** AAATGGGGCTACTTCAAGTTTTTACT	rs1569754, rs3946080, rs2143811, rs5772743
SDHB intron 1	**F –** GGTACATGATACCTTGGAGTGC **R –** ACCTCCCCTGTACTCCGTAAG	rs7545518, rs7545499, rs7536679

6. Penetrance of all Clinical Manifestations Related to *SDHB* Exon 1 Deletion

The penetrance for the different manifestations of the disease, such as PHEO, PGL, RCC or GIST, was estimated using the available clinical data from 78 *SDHB* exon 1 deletion carriers, including 22 probands and 56 family members. All estimates were calculated using the Kaplan-Meier method with IBM SPSS Statistics version 22 (SPSS inc., Chicago, IL). For probands and affected relatives, age was determined using the tumor diagnosis date. For unaffected relatives, the last follow-up date was used, being defined as the last normal biochemical screening carried out in the context of surveillance procedures. The penetrance estimation was performed including and excluding probands.

For comparison purposes, we also estimated the penetrance for the different manifestations of the disease in the families with other *SDHB* pathogenic variants. The penetrance estimation was performed using 17 probands and 30 family members.

IV. RESULTS

IV. Results

1. Characterization of Hereditary PPGL Families

The *SDHB* exon 1 deletion was confirmed in all 24 HPPGL, families identified at the Portuguese Oncology Institute of Porto. PGL was the most frequent tumor, representing about 76% (26/35) of all the tumors diagnosed in the families with the *SDHB* exon 1 deletion (Table 7). PHEO was the second most frequent tumor, representing about 14% (5/35) of all diagnosed tumors, followed by GIST diagnosed in about 6% (2/35) of the cases and RCC (1/35) and PA (1/35) diagnosed each in about 3% of the cases. Two pedigrees of two HPPGL families are shown in Figure 6. The mean age of PGL and PHEO diagnosis was approximately 37 years for both tumors (Table 7).

The geographic origin of the 24 HPPGL families studied at the Portuguese Oncology Institute of Porto was, for the majority of the cases, the north region of Portugal, especially Porto and Braga districts, with 7 and 14 families, respectively. The remaining families were from Viana do Castelo (two) and Lisbon (one) districts (Figure 7). Regarding the families from the Portuguese Institutes of Coimbra and Lisbon, two were originated from Coimbra and one each from Lisbon, Setúbal, Portalegre and Faro districts (Figure 7).

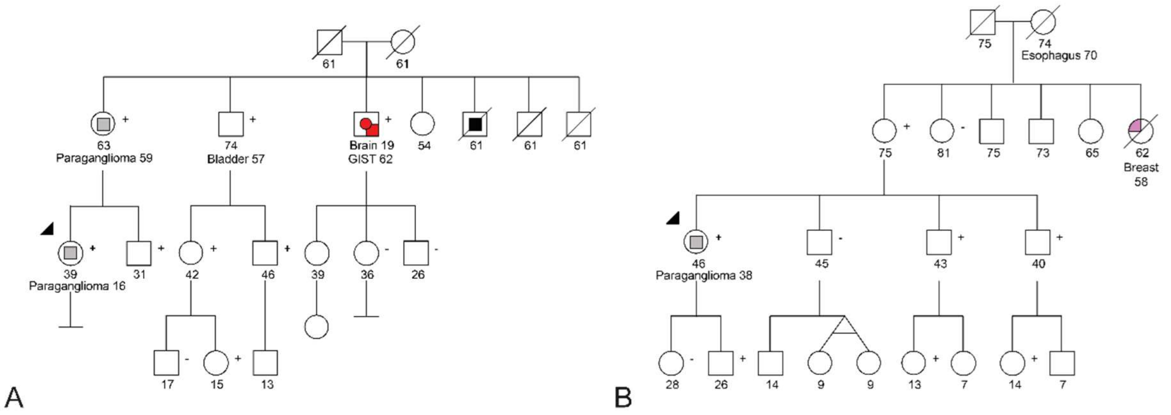
61
61
63
Paraganglioma 59
74
Bladder 57
Brain 19
GIST 62
54
61
61
61
39
Paraganglioma 16
31
42
46
39
36
26
17
15
13
A
75
74
Esophagus 70
75
81
75
73
65
62
Breast
58
46
Paraganglioma 38
45
43
40
28
26
14
9
9
13
7
14
7
B

Figure 6 - Pedigrees of two HPPGL families presenting the *SDHB* exon 1 deletion, namely family #7 (A) and family #8 (B).

Table 7 - Clinicopathological features of the 24 probands, studied at the Portuguese Oncology Institute of Porto, and 8 affected relatives.

Family	Kindred	Gender	Tumor type	Age at diagnosis	Geographic origin (district)
#1	Proband	F	Carotid-body PGL	39	Porto
#2	Proband	M	Paravertebral PGL	36	Porto
	Niece	F	PGL	8	
#3	Proband	M	Vesical PGL	35	Porto
	Brother	M	PHEO	55	
#4	Proband	M	Peritoneal PGL	28	Porto
	Mother	M	Carotid-body PGL	44	
#5	Proband	M	Cervical PGL	59	Braga
#6	Proband	M	Aortic PGL	19	Viana do Castelo
#7	Proband	F	Paravertebral PGL; Cervical PGL	16; 38	Porto
	Mother	F	Cervical PGL	51	
	Uncle	M	GIST	62	
	Brother	M	Jugulo-tympanic PGL	30	
#8	Proband	F	Carotid body PGL	38	Braga
#9	Proband	M	Paravertebral PGL	32	Braga
#10	Proband	[a]	[a]	[a]	Porto
#11	Proband	M	PHEO	40	Porto
#12	Proband	M	PHEO ; PA	15; 35	Braga
	Cousin	M	Carotid-body PGL	31	
#13	Proband	F	PHEO	14	Braga
#14	Proband	M	Jugular PGL	48	Braga
	Cousin	M	Jugulo-tympanic PGL	25	
	Uncle	M	GIST	61	
#15	Proband	F	Para-aortic PGL	22	Braga
#16	Proband	M	PGL[b]	15	Lisboa
#17	Proband	F	RCC	64	Braga
#18	Proband	F	Retroperitoneal PGL	41	Braga
#19	Proband	F	Cervical PGL	16	Braga
#20	Proband	M	Cervical PGL	[a]	Braga
#21	Proband	M	Abdominal PGL	68	Braga
#22	Proband	F	Cervical PGL & PHEO	61; 61	Viana do Castelo
#23	Proband	F	Retroperitoneal PGL	49	Braga
#24	Proband	F	Retroperitoneal PGL	33	Braga

PGL: Paraganglioma; PHEO: Pheochromocytoma; RCC: renal cell carcinoma; PA: Pituitary adenoma; GIST: Gastrointestinal stromal tumor. [a] No clinical information available. [b] No clinical information available related to the tumor anatomical location.

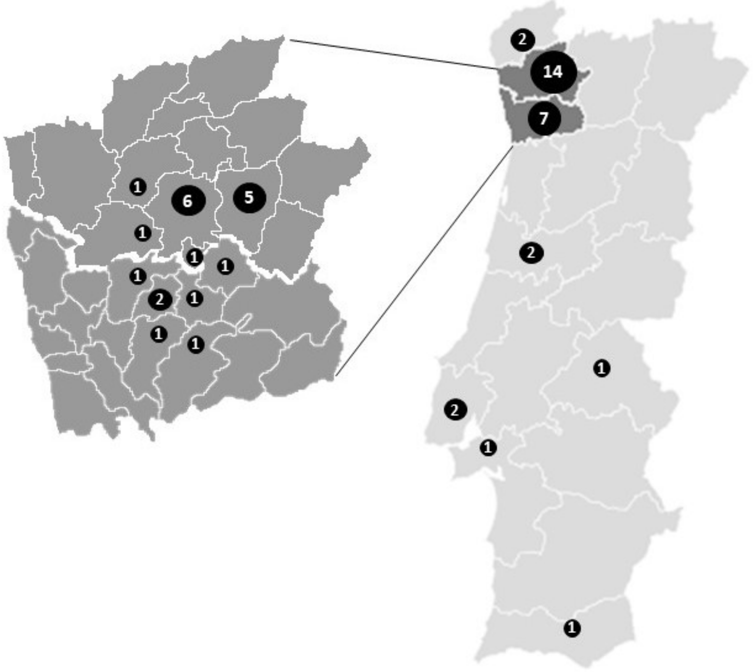

Figure 7 - Geographic origin of the families presenting the *SDHB* exon 1 germline deletion in Portugal. Black circles and the number within represent the families and its frequency. On the left, the larger-scale map represents Braga (upper) and Porto (lower) districts.

2. *SDHB* Exon 1 Deletion Breakpoint Identification and Characterization

The *SDHB* exon 1 deletion was confirmed in all the samples previously classified as positive by MLPA, either using the primers described by Solis et al. (2009) or the designed specific assay (Figure 8A). Furthermore, the results for the 27 negative cases were also concordant.

Sequence analysis of the mutated allele showed that all the samples harbored the 15 678 bp deletion previously described as an Iberian founder mutation (Cascon et al., 2008; Martins et al., 2013). This rearrangement comprises *SDHB* exon 1 and upstream 5' UTR region, being the 5' and 3' breakpoints located 10260 bp upstream *SDHB* 5' UTR region and 3865 bp upstream of *SDHB* exon 2, respectively. Therefore, the full description of the *SDHB* deletion is c.-151-10260_73-3865del (HGVS, NC_000001.11 (SDHB): ATG=1).

The 5' and 3' breakpoint flanking regions presented a complete homology sequence of 3 bp (CTG) (Figure 8B). The genomic sequences flanking the deletion breakpoints in *SDHB* 5' UTR region and intron 1 were analyzed for low-complexity DNA sequences and interspersed repeats and one AluSx repeat was found at intron 1 breakpoint. Within the upstream *SDHB* 5' UTR breakpoint, no *Alu* element was found, but an AluSx repeat was found in the flanking region near the breakpoint. These two *Alu* elements were highly homologous.

Additionally, we observed in all positive cases a deletion of four nucleotides (AATA) near the breakpoint region, corresponding to the *SDHB* variant LRG_316t1:c.73-3821_73-3818del (Figure 8B). This small deletion was not present in the wild-type allele of the carriers, nor in the non-carriers family members and normal controls cases.

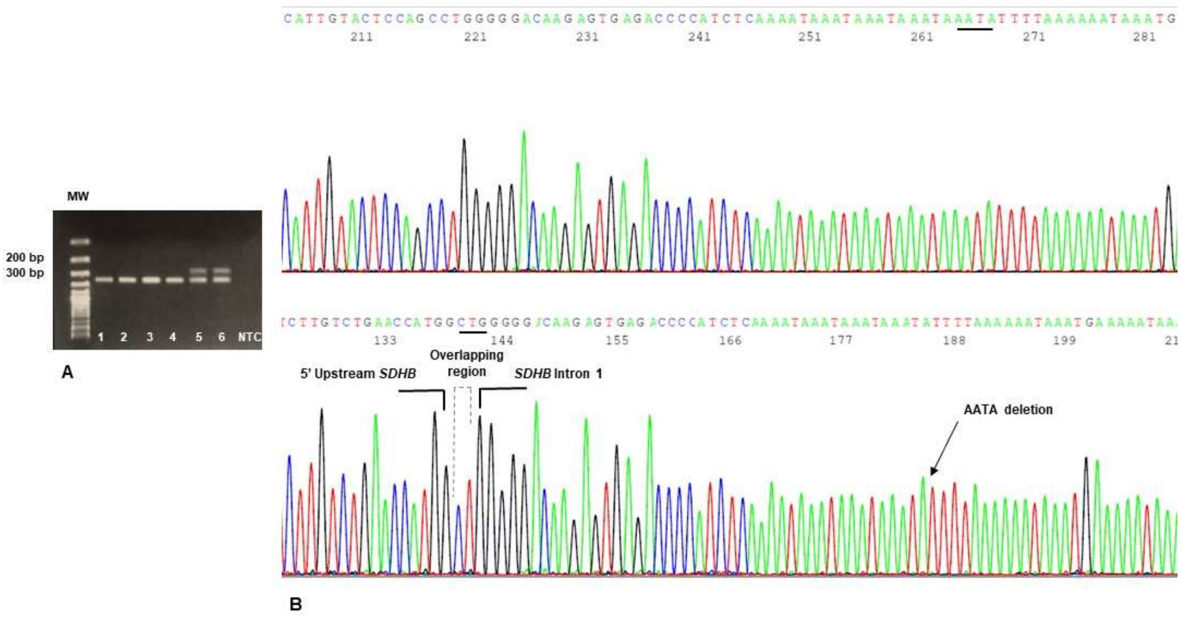

Figure 8 - Molecular characterization of the *SDHB* c.-151-10260_73-3865del mutation by a PCR specific assay and sequencing analysis. (A) Genomic DNA analysis by a three primer set amplification. The positive cases (lane 5 and 6) present two bands corresponding to a 351 bp amplicon from the wild-type allele and an additional 290 bp long amplicon from the mutated allele; the negative cases (lane 1 to 4) present only the 351 bp amplicon from the wild-type alleles. NTC is a non-template control and MW refers to 100 bp DNA standard. (B) Sequence electropherograms of the normal (upper) and mutated (lower) alleles in the *SDHB* exon 1 deletion breakpoint region. The overlapping region indicates a 3 bp homology sequence (CTG) shared by the 5' and 3' breakpoint flanking regions. The deletion of four nucleotides (AATA) in *SDHB* intron 1 is also indicated (black arrow).

3. Haplotype Analysis and Estimation of Mutation Age

Microsatellite haplotypes were phased for 12 out of the 30 Portuguese HPPGL families and 9 different haplotypes were observed (Table 8). Two haplotypes were more frequently observed, namely haplotype H1 and H7 present in three (families 5, 7 and 8) and two (families 10 and 14) families, respectively. The 12 informative families revealed a conserved region of about 47Kb, comprising the region between D1S170 microsatellite marker and the *SDHB* gene. Regarding the 12 families with unphased haplotypes, 10 families also harbored alleles consistent with the conserved region between the D1S170 marker and the *SDHB* gene (Table 8). Six families were excluded from the haplotype analysis due to inconclusive results.

The age estimation method that we planned to use takes into account the recombination rate (physical distance between the two most distant markers in cM), the microsatellite marker mutation rate and the average number of mutation and recombination events observed in the different haplotypes. The probability of mutation vs recombination is evaluated considering the minimum number of stepwise mutations required to explain the haplotype divergence from a single ancestor. For example, considering haplotype 1 (H1) the ancestral haplotype, the simplest explanation for the divergence observed in the haplotype 2 (H2) would be two recombination events, including markers D1S436 to D1S507 in the most telomeric region and markers D1S2644 to D1S2828 in the most centromeric region (Table 8). On the other hand, the divergence observed in haplotype 3 (H3) and 5 (H5) for marker D1S2826 is more difficult to explain given the observed conserved region that comprises markers D1S2644 and D1S2732 (Table 8). Given these doubts, we were not yet able to estimate the age of the mutation. However, SNP haplotypes will be constructed in order to establish whether a specific microsatellite is different from the consensus because of a recombination event rather than a mutation and the deletion age estimation will then be performed.

Regarding the SNP markers haplotyping, the 30 HPPGL families presented the same haplotype previously described by Martins et al. (2013) (Table 8).

4. Penetrance of all Manifestations Related to *SDHB* Exon 1 Deletion

Thirty (22 probands and 8 affected family members) of the 78 *SDHB* exon 1 deletion carriers presented a clinical manifestation of PPGL, RCC or GIST. The estimated penetrance, including probands, was 66.2% at the age of 75 years (Figure 9A). Excluding the probands, the estimated penetrance was 29.4% at the age of 75 years (Figure 9B). Regarding the group of the other *SDHB* pathogenic mutations, the estimated penetrance was 67.2% and 22.8% at the age of 75 years including and excluding the probands, respectively.

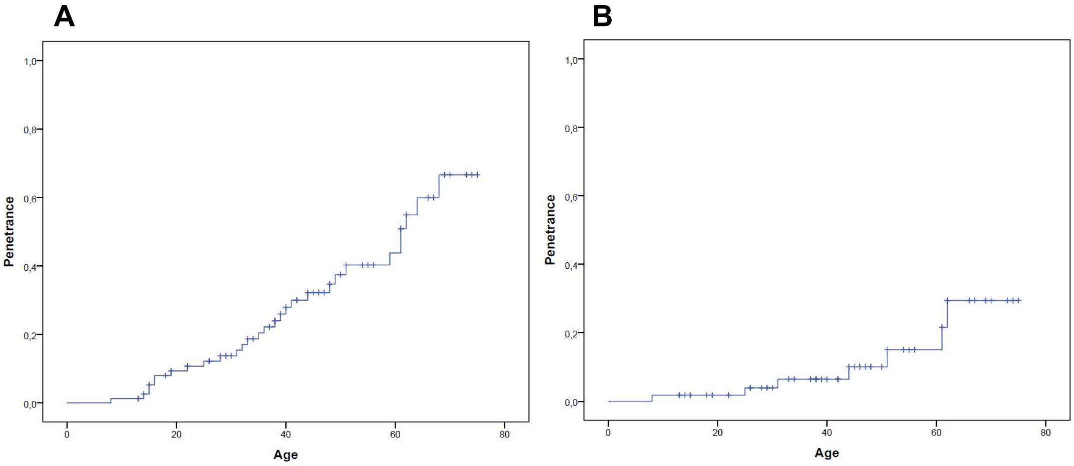

Figure 9 - Penetrance estimates of all manifestations (PPGLs, RCC and GIST) of the *SDHB* exon 1 deletion including probands (A) and excluding probands (B).

Table 8 - Microsatellite markers and SNP haplotypes of the 12 informative and 12 non-informative *SDHB* exon 1 deletion positive families.

Markers	**Families with phased haplotype**												**Non-informative families**											
	5 (H1)	**7 (H1)**	**8 (H1)**	**19 (H2)**	**3 (H3)**	**27 (H4)**	**25 (H5)**	**4 (H6)**	**14 (H7)**	**10 (H7)**	**1 (H8)**	**13 (H9)**	**24**	**29**	**15**	**22**	**9**	**6**	**20**	**28**	**16**	**30**	**18**	**23**
District of origin	BR	PO	BR	BR	PO	SE	CO	PO	BR	PO	PO	BR	BR	LI	BR	VC	BR	VC	BR	PA	LI	FA	BR	BR
tel																								
D1S507	186	186	186	184	192	198	186	184	184	184	188	188	184/188	196/198	196	184	186	186/196	186/196	186/202	192/196	192/196	196	186/196
D1S436	230	230	230	208	230	230	230	230	230	230	230	202	230	236	208/230	208	230	208/230	230/234	208/230	208/236	208	230/240	238
D1S170	218	218	218	218	218	218	218	218	218	218	218	218	218	228	218	218	218	218	218/222	204/218	228	218	218/228	218/222
rs1569754	C	C	C	C	C	C	C	C	C	C	C	C	C	C	C	C	C	C	C	C	C	C	C	C
rs3946080	A	A	A	A	A	A	A	A	A	A	A	A	A	A	A	A	A	A	A	A	A	A	A	A
rs2143811	C	C	C	C	C	C	C	C	C	C	C	C	C	C	C	C	C	C	C	C	C	C	C	C
SDHB	C	C	C	C	C	C	C	C	C	C	C	C	C	C	C	C	C	C	C	C	C	C	C	C
rs5772743	_A	_A	_A	_A	_A	_A	_A	_A	_A	_A	_A	_A	_A	_A	_A	_A	_A	_A	_A	_A	_A	_A	_A	_A
rs7545518	A	A	A	A	A	A	A	A	A	A	A	A	A	A	A	A	A	A	A	A	A	A	A	A
rs7545499	A	A	A	A	A	A	A	A	A	A	A	A	A	A	A	A	A	A	A	A	A	A	A	A
rs7536679	T	T	T	T	T	T	T	T	T	T	T	T	T	T	T	T	T	T	T	T	T	T	T	T
D1S2826	136	136	136	136	132	132	126	126	126	126	126	142	126	132	132	132	132/136	132	132	126	126/132	126/132	132/136	132/136
D1S2644	230	230	230	218	230	228	230	222	222	222	222	226	232	230	232	226/234	218	230/232	220/232	232	230	226/230	230	218/232
D1S2732	265	265	265	273	265	259	265	269	269	257	267	265	265	265	257	273	257	265/267	257/261	263	265	257	263/267	257/265
D1S2828	253	253	253	255	255	269	277	269	269	267	279	253	257	279	253	253	253	257/283	253/281	253/275	253	277/279	265/277	255/281
cen																								

(_A means deletion of an adenine nucleotide); (BR: Braga, FA: Faro, LI: Lisbon, PA: Portalegre, PO: Porto, SE: Setúbal, VC: Viana do Castelo)

V. DISCUSSION

V. Discussion

HPPGL can be caused by heterozygous germline variants in the genes that code for the four subunits and cofactor of the SDH mitochondrial enzyme, namely the *SDHA*, *SDHB*, *SDHC*, *SDHD* and *SDHAF2* genes (Benn et al., 2015). The mutational spectrum of the *SDHx* genes includes point mutations, small insertions and deletions, changes affecting splice sites and large genomic rearrangements, distributed throughout the genes (Fokkema et al., 2011). However, due to several founder effects, the spectrum of germline *SDHx* variants can differ greatly between countries. For example, the *SDHD* founder mutation c.274G>T plays a major role in the prevalence of HPPGL in the Netherlands (Hensen et al., 2012). Regarding *SDHB* gene*,* a deletion of exon three (c.201-4429_287-933del mutation) has also been described as a founder mutation in the Netherlands (Bayley et al., 2009; Rijken et al., 2016).

In 2004, a *SDHB* exon 1 germline deletion was identified in a Brazilian family with HPPGL (McWhinney et al., 2004). Afterward, *SDHB* exon 1 deletions were also described in three Spanish and one Portuguese families (Cascon et al., 2006; Cascon et al., 2008). Molecular characterization of these rearrangements revealed that they all harbored the same 15,678 bp deletion (Cascon et al., 2008). According to the authors, the four Iberian families were originated from a relatively small area of the northwest of the Iberian Peninsula, and haplotype analysis suggested a common ancestor, probably indicating a founder effect (Cascon et al., 2008). The *SDHB* 15,678 bp deletion was also described in one Spanish-Mexican descent family (Solis et al., 2009). More recently, Martins et al. (2013) identified this rearrangement in 11 families from the North of Portugal and SNP haplotype analysis showed that all the families shared a common haplotype, also suggesting a possible founder effect in northern Portuguese/Galician populations (Cascon et al., 2008; Solis et al., 2009; Martins et al., 2013).

Twenty-four families from the Portuguese Oncology Institute of Porto presented a *SDHB* exon 1 deletion, accounting for about 64% of all *SDHB* variants identified in families followed at this institution. Furthermore, several *SDHB* exon 1 deletions were identified at the Portuguese Oncology Institutes of Lisbon and Coimbra and, for the purpose of haplotype studies, we included in this study four and two families from these Institutions, respectively. Given the high frequency of the *SDHB* exon 1 deletion in Portugal, we aimed to evaluate if it is a founder mutation at national level. In order to do that, we first needed to perform the molecular characterization of all the deletions. Genomic breakpoint characterization showed that all the carriers presented the same 15,678 bp deletion previously described as a founder Iberian mutation (Cascon et al., 2008; Martins et al., 2013). Additionally, we observed a deletion of four nucleotides (AATA), located very close to the deletion breakpoint in all carriers. This small deletion was not observed in the wild-type allele of the carriers nor in the negative cases and normal controls analyzed. To our knowledge, this small deletion is not described in the literature or in variant databases. Additionally, none of the authors that studied the Iberian founder deletion reported this alteration (Cascon et al., 2006; Cascon et al., 2008; Solis et al., 2009; Martins et al., 2013). Given that this variant occurred near the breakpoint and would be detectable at least by the assay described by Solis et al. (2009), further studies including the Spanish samples would be needed to clarify this question. Nonetheless, the fact that all Portuguese carriers present this alteration is a strong indicator of a common origin. Haplotype analysis by microsatellite markers flanking the *SDHB* gene revealed a conserved region of about 47 kb in the 12 informative families. Furthermore, 12 non-informative families also harbored alleles consistent with the conserved region, indicating that these families could share a common ancestor. The haplotype divergence we observed can be explained by recombination and/or mutation events that accumulated in the ancestral haplotype. This variation accumulated in the ancestral haplotype can be used to estimate the age of the mutation (Martins et al., 2007). However, with the microsatellite haplotype results obtained so far, it is not yet possible to estimate the age of the *SDHB* exon 1 deletion.

Further haplotype studies including SNPs markers located in the regions that encompass the microsatellite markers will be performed to allow mutation age estimation. Regarding the SNPs haplotype previously described by Martins et al (2013), our results showed that all families shared the same reported haplotype (Martins et al., 2013). As indicated previously, a founder effect in northern Portuguese/Galician population was suggested because this rearrangement had not been described in Portuguese PPGL patients from central and southern Portugal (Domingues et al., 2012; Martins et al., 2013). Recently, Donato et al. (2019) reported eight HPPGL families, identified at the Portuguese Oncology Institute of Lisbon, with a *SDHB* exon 1 deletion, being one of the most frequent variants of their series (Donato et al., 2019). Furthermore, our study has shown that the *SDHB* exon 1 deletion presents a wider geographical distribution than previously reported. This deletion has been described only in countries with strong historical links with Portugal and Spain, either by colonization processes (from Portugal to Brazil and from Spain to Mexico) or more recent emigration flows (from Portugal to Brazil) (Sousa et al., 2007; Arruda et al., 2013; Izquierdo et al., 2015). However, given that several deletions affecting *SDHB* exon 1 have been reported worldwide, without genomic breakpoints determination, this deletion could also be present in other countries. Further studies including all the reported families worldwide would be needed to evaluate the ancestral origin of this mutation. Nonetheless, to our knowledge this is the first study to perform an extensive microsatellite haplotype analysis in *SDHB* exon 1 deletion carriers, demonstrating that the majority of the Portuguese families share a longer conserved region than the previously reported by Martins et al., (2013), further supporting the hypothesis of a founder mutation (Martins et al., 2013).

On the other hand, we cannot exclude the possibility that the *SDHB* exon 1 deletion could have occurred several times *de novo.* Considering that it could be a recurrent rearrangement, this region may be a hot spot for large genomic rearrangements, as previously suggested by Cascon et al. (2006). According to these authors, the *SDHB* intron 1 presents a high density of *Alu* repeats, comprising 36% of the region (Cascon et al., 2006). *Alu* elements are retrotransposable interspersed repetitive sequences that belong to a class of elements named short interspersed nuclear elements (SINEs), and account for approximately 11% of the human genome (Deininger, 2011; Kim et al., 2016). *Alu* elements are a major cause of non-allelic homologous recombination (NAHR) events causing large genomic rearrangements and disease (Kolomietz et al., 2002; Kim et al., 2016). As previously indicated, an *Alu* repeat was found only at the *SDHB* intron 1 breakpoint (AluSx) (Cascon et al., 2006). However, we also observed an AluSx repeat near the upstream *SDHB* 5' UTR breakpoint that is highly homologous to the one observed at intron 1. Therefore, we cannot exclude NAHR mediated by *Alu* elements as a possible mechanism for the occurrence of this rearrangement. Alternatively, Cascon et al. (2008) observed, at the breakpoint region, a DNA sequence motif known to be associated with site-specific recombination, mutation, cleavage and gene rearrangements (the DNA polymerase α frameshift hotspot GGGGGA) (Abeysinghe et al., 2003) and suggested that the mechanism involved in *SDHB* exon 1 deletion was different from *Alu*-mediated genomic recombination (Cascon et al., 2008). As indicated previously, a four base deletion was observed near the breakpoint junction and located in one short tandem repeat sequence. According to Esposito et al (2017), genomic rearrangements can give rise to microdeletions, generally located in palindromic and repeat sequences (Esposito et al., 2017). The authors suggest that these types of sequences may promote DNA instability, predisposing these regions to DNA breakage and recombination (Esposito et al., 2017). Therefore, one possible explanation for the observed small deletion is that it resulted from the mechanism responsible for this rearrangement.

Regarding the phenotype of the 24 HPPGL families, we observed that PGL was more frequently diagnosed than PHEO (74% versus 14%, respectively). This result is in accordance with previous studies, in which families presenting *SDHB* mutations showed a predominant clinical phenotype of PGL (Burnichon et al., 2009; Martins et al., 2013; Gunawardane and Grossman, 2017). Regarding the PGLs anatomical location, thoracic-abdominal location was more frequently observed when compared to head-and-neck location, which it is also concordant with the literature (Gunawardane and Grossman, 2017). The mean age at diagnosis reported in the literature (30 years) is also in concordance with our results (37 years) (Gunawardane and Grossman, 2017). Additionally, when we compare with the group of the remaining *SDHB* pathogenic mutations identified at our institution, the mean age at diagnosis was similar (39 years) and PGL was also the most frequent tumor diagnosed in these families.

Although with a much lower prevalence, we observed the presence of other types of tumors previously associated with *SDHB* germline mutations, namely RCC, PA and GIST (Benn et al., 2015; Evenepoel et al., 2015; Gill, 2018; Muth et al., 2019). RCC belongs to the tumor spectrum of PGL type 4, occurring in approximately 14% of the cases, and in some families it has been reported as the only clinical phenotype (Benn et al., 2015). Regarding PA, although associated with mutations in the *SDHx* genes, it is rarely diagnosed in the context of HPPGL, being mainly described in case reports and small series (Benn et al., 2015; Xekouki et al., 2015; Gill, 2018). GISTs are the most common type of mesenchymal gastrointestinal tumors, usually associated with somatic activating mutations in *KIT* or *PDGFRA* genes (Wang et al., 2015). A small subset of GISTs is associated with SDH deficiency (Wang et al., 2015), due to germline mutations in *SDHx* genes (Gill, 2018). For example, the Carney-Stratakis syndrome is characterized by the occurrence of gastric GIST and PGL, due to germline mutations in the *SDHx* genes (Wang et al., 2015).

Penetrance is defined as the proportion of individuals with a given genotype who exhibit the phenotype associated to that genotype. PPGLs associated with mutations in *SDHB* are characterized by a high risk of malignancy, so estimating the age-dependent penetrance of these alterations is extremely important. The apparent age-related penetrance for *SDHB* mutation carriers varies widely in the literature, ranging from 9% to 77% at 50 years of age (Neumann et al., 2004; Hes et al., 2010; Rijken et al., 2016; Andrews et al., 2018; Rijken et al., 2018). The observed difference in disease penetrance across studies is mainly due to the method, size and type of cohorts used in penetrance estimation. While initial studies used cohorts of symptomatic PPGL patients (mostly probands) and a limited number of asymptomatic family members, more recent studies tend to exclude probands from the analysis. Although the estimates obtained from studies that include probands can overestimate the penetrance, exclusion of affected patients from the analysis can also be prone to bias in low-penetrant diseases, because it discards valuable information of affected mutation carriers (Andrews et al., 2018; Rijken et al., 2018). Adequate methodologies for penetrance calculations must be used in order to correct for these ascertainment bias. Regardless of these, penetrance estimates for *SDHB* mutation carriers have decreased since the first reports. According to two recent studies, from the Netherlands and United Kingdom, the estimated penetrance of *SDHB* mutations was 21%

and 16% by age 50 years, respectively (Andrews et al., 2018; Rijken et al., 2018). Concerning *SDHB* exon 1 deletions, Jochmanova et al. (2017) estimated the penetrance of 31 carriers (including probands) of the c.1-16418_73-5173del rearrangement to be 50% at 63 years of age. Solis et al. (2009) also estimated the penetrance on a large family with the *SDHB* 15,678 bp Iberian founder deletion and obtained a value of 35% at 40 years of age. As expected, the estimated penetrance observed in our work was higher when we included the probands in the analysis (66.2% and 29.4% at the age of 75 years, including and excluding probands, respectively). Our study also suggests a lower penetrance when compared with that estimated by Solis et al. (2009). The difference observed could be due to the size of the series, given that they only included in the analysis 23 mutation carriers. On the other hand, our estimated disease penetrance in non-proband *SDHB* mutation carriers is in accordance with recent studies regarding other mutations in *SDHB* gene, in which the estimated penetrance is lower than the previously reported (Schiavi et al., 2010; Andrews et al., 2018; Rijken et al., 2018). Additionally, the estimated penetrance of all the remaining *SDHB* pathogenic mutations of our series was similar to the one observed for the *SDHB* exon 1 deletion. Further studies including all the families that present the *SDHB* exon 1 founder mutation could help to determine with more accuracy the penetrance of this rearrangement. Be that as it may, we have currently no evidence that the penetrance of this founder *SDHB* deletion is different from that of other *SDHB* mutations.

VI. CONCLUSIONS

VI. Conclusions

The main conclusions of this thesis are:

- All *SDHB* exon 1 deletion carriers presented the same 15,678 bp deletion previously described as the Iberian founder deletion, as well as a previously unreported 4 bp deletion nearby the breakpoint;
- The extensive haplotype analysis with microsatellite markers showed a conserved region of 47 kb suggesting a common ancestor for all Portuguese families, but further studies are needed to estimate the *SDHB* exon 1 deletion age;
- Evaluation of the geographic origin of the families revealed that the majority of the *SDHB* deletion carriers are from the north region of Portugal, but that it also exists in families originating from other regions of the country;
- The penetrance of this founder *SDHB* deletion is similar to that observed for other *SDHB* mutations.

VII. FUTURE PERSPECTIVES

VII. Future Perspectives

In order to support and improve our results and conclusions, we plan to:

- Determine if the genomic breakpoints of all *SDHB* exon 1 deletions described worldwide are the same as those of the Iberian founder deletion, as well as to confirm if all carriers have the nearby 4 bp deletion we identified in this study;
- Perform additional haplotype studies, including more SNPs markers, in all families with the Iberian founder deletion reported worldwide;
- Estimate the age of the Iberian Peninsula deletion, using the information obtained from microsatellite and SNPs extended haplotyping;
- Perform additional penetrance studies including all the reported carriers of the Iberian Peninsula deletion as compared with other deleterious *SDHB* variants.

VIII. REFERENCES

VIII. References

Abeysinghe, S. S., Chuzhanova, N., Krawczak, M., Ball, E. V., & Cooper, D. N. (2003). Translocation and gross deletion breakpoints in human inherited disease and cancer I: Nucleotide composition and recombination-associated motifs. In *Hum Mutat* (2003/08/26 ed., Vol. 22, pp. 229-244).

Aldera, A. P., & Govender, D. (2018). Gene of the month: SDH. In *J Clin Pathol* (2017/10/27 ed., Vol. 71, pp. 95-97).

Amar, L., Baudin, E., Burnichon, N., Peyrard, S., Silvera, S., Bertherat, J.*, et al.* (2007). Succinate dehydrogenase B gene mutations predict survival in patients with malignant pheochromocytomas or paragangliomas. In *J Clin Endocrinol Metab* (2007/07/27 ed., Vol. 92, pp. 3822-3828).

Andrews, K. A., Ascher, D. B., Pires, D. E. V., Barnes, D. R., Vialard, L., Casey, R. T.*, et al.* (2018). Tumour risks and genotype-phenotype correlations associated with germline variants in succinate dehydrogenase subunit genes SDHB, SDHC and SDHD. In *J Med Genet* (2018/02/02 ed., Vol. 55, pp. 384-394).

Arruda, J., Ferlini, V., Matos, M., & Sousa, F. (2013). *De colonos a imigrantes: i(E)migração portuguesa para o brasil.* (Alameda Ed.). São Paulo, Brasil.

Astrom, K., Cohen, J. E., Willett-Brozick, J. E., Aston, C. E., & Baysal, B. E. (2003). Altitude is a phenotypic modifier in hereditary paraganglioma type 1: evidence for an oxygen-sensing defect. In *Hum Genet* (2003/06/18 ed., Vol. 113, pp. 228-237).

Astuti, D., Latif, F., Dallol, A., Dahia, P. L., Douglas, F., George, E.*, et al.* (2001). Gene mutations in the succinate dehydrogenase subunit SDHB cause susceptibility to familial pheochromocytoma and to familial paraganglioma. In *Am J Hum Genet* (2001/06/19 ed., Vol. 69, pp. 49-54).

Bardella, C., Pollard, P. J., & Tomlinson, I. (2011). SDH mutations in cancer. In *Biochim Biophys Acta* (2011/07/21 ed., Vol. 1807, pp. 1432-1443).

Bayley, J. P., Grimbergen, A. E., van Bunderen, P. A., van der Wielen, M., Kunst, H. P., Lenders, J. W.*, et al.* (2009). The first Dutch SDHB founder deletion in paraganglioma-pheochromocytoma patients. In *BMC Med Genet* (2009/04/17 ed., Vol. 10, pp. 34).

Bayley, J. P., Oldenburg, R. A., Nuk, J., Hoekstra, A. S., van der Meer, C. A., Korpershoek, E.*, et al.* (2014). Paraganglioma and pheochromocytoma upon maternal transmission of SDHD mutations. In *BMC Med Genet* (2014/10/11 ed., Vol. 15, pp. 111).

Baysal, B. E., Ferrell, R. E., Willett-Brozick, J. E., Lawrence, E. C., Myssiorek, D., Bosch, A.*, et al.* (2000). Mutations in SDHD, a mitochondrial complex II gene, in hereditary paraganglioma. In *Science* (2000/02/05 ed., Vol. 287, pp. 848-851).

Benn, D. E., Gimenez-Roqueplo, A. P., Reilly, J. R., Bertherat, J., Burgess, J., Byth, K.*, et al.* (2006). Clinical presentation and penetrance of pheochromocytoma/paraganglioma syndromes. In *J Clin Endocrinol Metab* (2005/12/01 ed., Vol. 91, pp. 827-836).

Benn, D. E., Robinson, B. G., & Clifton-Bligh, R. J. (2015). 15 YEARS OF PARAGANGLIOMA: Clinical manifestations of paraganglioma syndromes types 1-5. In *Endocr Relat Cancer* (2015/08/15 ed., Vol. 22, pp. T91-103).

Bennedbaek, M., Rossing, M., Rasmussen, A. K., Gerdes, A. M., Skytte, A. B., Jensen, U. B.*, et al.* (2016). Identification of eight novel SDHB, SDHC, SDHD germline variants in Danish pheochromocytoma/paraganglioma patients. In *Hered Cancer Clin Pract* (2016/06/10 ed., Vol. 14, pp. 13).

Benson, G. (1999). Tandem repeats finder: a program to analyze DNA sequences. In *Nucleic Acids Res* (1998/12/24 ed., Vol. 27, pp. 573-580).

Berends, A. M. A., Buitenwerf, E., de Krijger, R. R., Veeger, N., van der Horst-Schrivers, A. N. A., Links, T. P.*, et al.* (2018). Incidence of pheochromocytoma and sympathetic paraganglioma in the Netherlands: A nationwide study and systematic review. In *Eur J Intern Med* (2018/01/24 ed., Vol. 51, pp. 68-73).

Berruti, A., Baudin, E., Gelderblom, H., Haak, H. R., Porpiglia, F., Fassnacht, M.*, et al.* (2012). Adrenal cancer: ESMO Clinical Practice Guidelines for diagnosis, treatment and follow-up. In *Ann Oncol* (2012/11/20 ed., Vol. 23 Suppl 7, pp. vii131-138).

Bielinska, M., Parviainen, H., Kiiveri, S., Heikinheimo, M., & Wilson, D. B. (2009). Review paper: origin and molecular pathology of adrenocortical neoplasms. In *Vet Pathol* (2009/03/06 ed., Vol. 46, pp. 194-210).

Boedeker, C. C., Erlic, Z., Richard, S., Kontny, U., Gimenez-Roqueplo, A. P., Cascon, A.*, et al.* (2009). Head and neck paragangliomas in von Hippel-Lindau disease and multiple endocrine neoplasia type 2. In *J Clin Endocrinol Metab* (2009/04/02 ed., Vol. 94, pp. 1938-1944).

Boikos, S. A., Pappo, A. S., Killian, J. K., LaQuaglia, M. P., Weldon, C. B., George, S.*, et al.* (2016). Molecular Subtypes of KIT/PDGFRA Wild-Type Gastrointestinal Stromal Tumors: A Report From the National Institutes of Health Gastrointestinal Stromal Tumor Clinic. In *JAMA Oncol* (2016/03/25 ed., Vol. 2, pp. 922-928).

Brandi, M. L., Gagel, R. F., Angeli, A., Bilezikian, J. P., Beck-Peccoz, P., Bordi, C.*, et al.* (2001). Guidelines for diagnosis and therapy of MEN type 1 and type 2. In *J Clin Endocrinol Metab* (2001/12/12 ed., Vol. 86, pp. 5658-5671).

Bray, F., Ferlay, J., Soerjomataram, I., Siegel, R. L., Torre, L. A., & Jemal, A. (2018). Global cancer statistics 2018: GLOBOCAN estimates of incidence and mortality worldwide for 36 cancers in 185 countries. In *CA Cancer J Clin* (2018/09/13 ed., Vol. 68, pp. 394-424).

Buffet, A., Smati, S., Mansuy, L., Menara, M., Lebras, M., Heymann, M. F.*, et al.* (2014). Mosaicism in HIF2A-related polycythemia-paraganglioma syndrome. In *J Clin Endocrinol Metab* (2013/11/28 ed., Vol. 99, pp. E369-373).

Buffet, A., Venisse, A., Nau, V., Roncellin, I., Boccio, V., Le Pottier, N.*, et al.* (2012). A decade (2001-2010) of genetic testing for pheochromocytoma and paraganglioma. In *Horm Metab Res* (2012/04/21 ed., Vol. 44, pp. 359-366).

Burnichon, N., Briere, J. J., Libe, R., Vescovo, L., Riviere, J., Tissier, F.*, et al.* (2010). SDHA is a tumor suppressor gene causing paraganglioma. In *Hum Mol Genet* (2010/05/21 ed., Vol. 19, pp. 3011-3020).

Burnichon, N., Rohmer, V., Amar, L., Herman, P., Leboulleux, S., Darrouzet, V.*, et al.* (2009). The succinate dehydrogenase genetic testing in a large prospective series of patients with paragangliomas. In *J Clin Endocrinol Metab* (2009/05/21 ed., Vol. 94, pp. 2817-2827).

References

Cascon, A., Comino-Mendez, I., Curras-Freixes, M., de Cubas, A. A., Contreras, L., Richter, S.*, et al.* (2015). Whole-exome sequencing identifies MDH2 as a new familial paraganglioma gene. In *J Natl Cancer Inst* (2015/03/15 ed., Vol. 107).

Cascon, A., Landa, I., Lopez-Jimenez, E., Diez-Hernandez, A., Buchta, M., Montero-Conde, C.*, et al.* (2008). Molecular characterisation of a common SDHB deletion in paraganglioma patients. In *J Med Genet* (2007/12/07 ed., Vol. 45, pp. 233-238).

Cascon, A., Montero-Conde, C., Ruiz-Llorente, S., Mercadillo, F., Leton, R., Rodriguez-Antona, C.*, et al.* (2006). Gross SDHB deletions in patients with paraganglioma detected by multiplex PCR: a possible hot spot? In *Genes Chromosomes Cancer* (2005/11/01 ed., Vol. 45, pp. 213-219).

Cascon, A., Pita, G., Burnichon, N., Landa, I., Lopez-Jimenez, E., Montero-Conde, C.*, et al.* (2009). Genetics of pheochromocytoma and paraganglioma in Spanish patients. In *J Clin Endocrinol Metab* (2009/03/05 ed., Vol. 94, pp. 1701-1705).

Cascon, A., Remacha, L., Calsina, B., & Robledo, M. (2019). Pheochromocytomas and Paragangliomas: Bypassing Cellular Respiration. In *Cancers (Basel)* (2019/05/19 ed., Vol. 11).

Castro-Vega, L. J., Buffet, A., De Cubas, A. A., Cascon, A., Menara, M., Khalifa, E.*, et al.* (2014). Germline mutations in FH confer predisposition to malignant pheochromocytomas and paragangliomas. In *Hum Mol Genet* (2013/12/18 ed., Vol. 23, pp. 2440-2446).

Castro-Vega, L. J., Lepoutre-Lussey, C., Gimenez-Roqueplo, A. P., & Favier, J. (2016). Rethinking pheochromocytomas and paragangliomas from a genomic perspective. In *Oncogene* (2015/06/02 ed., Vol. 35, pp. 1080-1089).

Cerecer-Gil, N. Y., Figuera, L. E., Llamas, F. J., Lara, M., Escamilla, J. G., Ramos, R.*, et al.* (2010). Mutation of SDHB is a cause of hypoxia-related high-altitude paraganglioma. In *Clin Cancer Res* (2010/07/02 ed., Vol. 16, pp. 4148-4154).

Chan JKC, Kimura N, Capella C, Gill A, Komminoth P, Lam AKY*, et al.* (2017). Paraganglion tumours. In L. IARC (Ed.), *WHO classification of head and neck tumours.* (4th ed., pp. 275–284).

Cilliers, D., Park, S., Sarson, K., Kenwrick, S., Simpson, H., Bradley, L., *et al.* (2013). A Family with Co-existing SDHB and SDHD Mutations Causing Hereditary Paraganglioma Syndrome. In *American Journals of Cancer Case Reports* (Vol. 1).

Comino-Mendez, I., Gracia-Aznarez, F. J., Schiavi, F., Landa, I., Leandro-Garcia, L. J., Leton, R., *et al.* (2011). Exome sequencing identifies MAX mutations as a cause of hereditary pheochromocytoma. In *Nat Genet* (2011/06/21 ed., Vol. 43, pp. 663-667).

Crossey, P. A., Richards, F. M., Foster, K., Green, J. S., Prowse, A., Latif, F., *et al.* (1994). Identification of intragenic mutations in the von Hippel-Lindau disease tumour suppressor gene and correlation with disease phenotype. In *Hum Mol Genet* (1994/08/01 ed., Vol. 3, pp. 1303-1308).

Dackiw, A. P., Cote, G. J., Fleming, J. B., Schultz, P. N., Stanford, P., Vassilopoulou-Sellin, R., *et al.* (1999). Screening for MEN1 mutations in patients with atypical endocrine neoplasia. In *Surgery* (1999/12/22 ed., Vol. 126, pp. 1097-1103; discussion 1103-1094).

Dahia, P. L. (2014). Pheochromocytoma and paraganglioma pathogenesis: learning from genetic heterogeneity. In *Nat Rev Cancer* (2014/01/21 ed., Vol. 14, pp. 108-119).

Deininger, P. (2011). Alu elements: know the SINEs. In *Genome Biol* (2011/12/30 ed., Vol. 12, pp. 236).

Delman, K. A., Shapiro, S. E., Jonasch, E. W., Lee, J. E., Curley, S. A., Evans, D. B., *et al.* (2006). Abdominal visceral lesions in von Hippel-Lindau disease: incidence and clinical behavior of pancreatic and adrenal lesions at a single center. In *World J Surg* (2006/04/18 ed., Vol. 30, pp. 665-669).

Domingues, R., Montalvao, P., Magalhaes, M., Santos, R., Duarte, L., & Bugalho, M. J. (2012). Identification of three new variants of SDHx genes in a cohort of Portuguese patients with extra-adrenal paragangliomas. In *J Endocrinol Invest* (2012/02/02 ed., Vol. 35, pp. 975-980).

Donato, S., Simoes, H., Pinto, A. T., B, M. C., & Leite, V. (2019). SDHx-related pheochromocytoma/paraganglioma - genetic, clinical, and treatment outcomes in a series of 30 patients from a single center. In *Endocrine* (2019/05/20 ed., Vol. 65, pp. 408-415).

References

Eisenhofer, G., Goldstein, D. S., Sullivan, P., Csako, G., Brouwers, F. M., Lai, E. W., *et al.* (2005). Biochemical and clinical manifestations of dopamine-producing paragangliomas: utility of plasma methoxytyramine. In *J Clin Endocrinol Metab* (2005/01/13 ed., Vol. 90, pp. 2068-2075).

Eisenhofer, G., Timmers, H. J., Lenders, J. W., Bornstein, S. R., Tiebel, O., Mannelli, M., *et al.* (2011). Age at diagnosis of pheochromocytoma differs according to catecholamine phenotype and tumor location. In *J Clin Endocrinol Metab* (2010/12/15 ed., Vol. 96, pp. 375-384).

Else, T., Greenberg, S., & Fishbein, L. (2018). Hereditary Paraganglioma-Pheochromocytoma Syndromes. In M. P. Adam, H. H. Ardinger, R. A. Pagon, S. E. Wallace, L. J. H. Bean, K. Stephens, & A. Amemiya (Eds.), *GeneReviews((R))*. Seattle (WA).

Erickson, D., Kudva, Y. C., Ebersold, M. J., Thompson, G. B., Grant, C. S., van Heerden, J. A., *et al.* (2001). Benign paragangliomas: clinical presentation and treatment outcomes in 236 patients. In *J Clin Endocrinol Metab* (2001/11/10 ed., Vol. 86, pp. 5210-5216).

Esposito, G., Tremolaterra, M. R., Marsocci, E., Tandurella, I. C., Fioretti, T., Savarese, M., *et al.* (2017). Precise mapping of 17 deletion breakpoints within the central hotspot deletion region (introns 50 and 51) of the DMD gene. In *J Hum Genet* (2017/09/08 ed., Vol. 62, pp. 1057-1063).

Evenepoel, L., Papathomas, T. G., Krol, N., Korpershoek, E., de Krijger, R. R., Persu, A., *et al.* (2015). Toward an improved definition of the genetic and tumor spectrum associated with SDH germ-line mutations. In *Genet Med* (2014/11/14 ed., Vol. 17, pp. 610-620).

Favier, J., Amar, L., & Gimenez-Roqueplo, A. P. (2015). Paraganglioma and phaeochromocytoma: from genetics to personalized medicine. In *Nat Rev Endocrinol* (2014/11/12 ed., Vol. 11, pp. 101-111).

Favier, J., & Gimenez-Roqueplo, A. P. (2010). Pheochromocytomas: the (pseudo)-hypoxia hypothesis. In *Best Pract Res Clin Endocrinol Metab* (2010/12/01 ed., Vol. 24, pp. 957-968).

Ferlay, J., Colombet, M., Soerjomataram, I., Mathers, C., Parkin, D. M., Pineros, M.*, et al.* (2019). Estimating the global cancer incidence and mortality in 2018: GLOBOCAN sources and methods. In *Int J Cancer* (2018/10/24 ed., Vol. 144, pp. 1941-1953).

Ferner, R. E., Huson, S. M., Thomas, N., Moss, C., Willshaw, H., Evans, D. G.*, et al.* (2007). Guidelines for the diagnosis and management of individuals with neurofibromatosis 1. In *J Med Genet* (2006/11/16 ed., Vol. 44, pp. 81-88).

Fishbein, L. (2019). Pheochromocytoma/Paraganglioma: Is This a Genetic Disorder? In *Curr Cardiol Rep* (2019/08/02 ed., Vol. 21, pp. 104).

Fishbein, L., Leshchiner, I., Walter, V., Danilova, L., Robertson, A. G., Johnson, A. R.*, et al.* (2017). Comprehensive Molecular Characterization of Pheochromocytoma and Paraganglioma. In *Cancer Cell* (2017/02/07 ed., Vol. 31, pp. 181-193).

Fishbein, L., & Nathanson, K. L. (2012). Pheochromocytoma and paraganglioma: understanding the complexities of the genetic background. In *Cancer Genet* (2012/03/21 ed., Vol. 205, pp. 1-11).

Fokkema, I. F., Taschner, P. E., Schaafsma, G. C., Celli, J., Laros, J. F., & den Dunnen, J. T. (2011). LOVD v.2.0: the next generation in gene variant databases. In *Hum Mutat* (2011/04/27 ed., Vol. 32, pp. 557-563).

Fowler, A., Mahamdallie, S., Ruark, E., Seal, S., Ramsay, E., Clarke, M.*, et al.* (2016). Accurate clinical detection of exon copy number variants in a targeted NGS panel using DECoN. In *Wellcome Open Res* (2017/05/02 ed., Vol. 1, pp. 20).

Gill, A. J. (2018). Succinate dehydrogenase (SDH)-deficient neoplasia. In *Histopathology* (2017/12/15 ed., Vol. 72, pp. 106-116).

Gill, A. J., Pachter, N. S., Clarkson, A., Tucker, K. M., Winship, I. M., Benn, D. E.*, et al.* (2011). Renal tumors and hereditary pheochromocytoma-paraganglioma syndrome type 4. In *N Engl J Med* (2011/03/04 ed., Vol. 364, pp. 885-886).

Gill, A. J., Toon, C. W., Clarkson, A., Sioson, L., Chou, A., Winship, I.*, et al.* (2014). Succinate dehydrogenase deficiency is rare in pituitary adenomas. In *Am J Surg Pathol* (2014/03/15 ed., Vol. 38, pp. 560-566).

Gottlieb, E., & Tomlinson, I. P. (2005). Mitochondrial tumour suppressors: a genetic and biochemical update. In *Nat Rev Cancer* (2005/12/06 ed., Vol. 5, pp. 857-866).

References

Gruber, & Simon, M. C. (2006). Hypoxia-inducible factors, hypoxia, and tumor angiogenesis. In *Curr Opin Hematol* (2006/03/29 ed., Vol. 13, pp. 169-174).

Gruber, L. M., Erickson, D., Babovic-Vuksanovic, D., Thompson, G. B., Young, W. F., Jr., & Bancos, I. (2017). Pheochromocytoma and paraganglioma in patients with neurofibromatosis type 1. In *Clin Endocrinol (Oxf)* (2016/07/28 ed., Vol. 86, pp. 141-149).

Guerrero-Perez, F., Fajardo, C., Torres Vela, E., Gimenez-Palop, O., Lisbona Gil, A., Martin, T., *et al.* (2019). 3P association (3PAs): Pituitary adenoma and pheochromocytoma/paraganglioma. A heterogeneous clinical syndrome associated with different gene mutations. In *Eur J Intern Med* (2019/08/23 ed.).

Gunawardane, P. T., & Grossman, A. (2017). The clinical genetics of phaeochromocytoma and paraganglioma. In *Arch Endocrinol Metab* (2017/11/23 ed., Vol. 61, pp. 490-500).

Gupta, G., Pacak, K., & Committee, A. A. S. (2017). Precision Medicine: An Update on Genotype/Biochemical Phenotype Relationships in Pheochromocytoma/Paraganglioma Patients. In *Endocr Pract* (2017/03/24 ed., Vol. 23, pp. 690-704).

Gyapay, G., Morissette, J., Vignal, A., Dib, C., Fizames, C., Millasseau, P., *et al.* (1994). The 1993-94 Genethon human genetic linkage map. In *Nat Genet* (1994/06/01 ed., Vol. 7, pp. 246-339).

Hanahan, D., & Weinberg, R. A. (2011). Hallmarks of cancer: the next generation. In *Cell* (2011/03/08 ed., Vol. 144, pp. 646-674).

Hannah-Shmouni, F., Pacak, K., & Stratakis, C. A. (2017). Metanephrines for Evaluating Palpitations and Flushing. In *JAMA* (2017/07/26 ed., Vol. 318, pp. 385-386).

Hao, H. X., Khalimonchuk, O., Schraders, M., Dephoure, N., Bayley, J. P., Kunst, H., *et al.* (2009). SDH5, a gene required for flavination of succinate dehydrogenase, is mutated in paraganglioma. In *Science* (2009/07/25 ed., Vol. 325, pp. 1139-1142).

Hensen, E. F., van Duinen, N., Jansen, J. C., Corssmit, E. P., Tops, C. M., Romijn, J. A., *et al.* (2012). High prevalence of founder mutations of the succinate dehydrogenase genes in the Netherlands. In *Clin Genet* (2011/02/26 ed., Vol. 81, pp. 284-288).

Hes, F. J., Weiss, M. M., Woortman, S. A., de Miranda, N. F., van Bunderen, P. A., Bonsing, B. A.*, et al.* (2010). Low penetrance of a SDHB mutation in a large Dutch paraganglioma family. In *BMC Med Genet* (2010/06/15 ed., Vol. 11, pp. 92).

Hoekstra, A. S., van den Ende, B., Julia, X. P., van Breemen, L., Scheurwater, K., Tops, C. M.*, et al.* (2017). Simple and rapid characterization of novel large germline deletions in SDHB, SDHC and SDHD-related paraganglioma. In *Clin Genet* (2016/08/04 ed., Vol. 91, pp. 536-544).

Isaacs, J. S., Jung, Y. J., Mole, D. R., Lee, S., Torres-Cabala, C., Chung, Y. L.*, et al.* (2005). HIF overexpression correlates with biallelic loss of fumarate hydratase in renal cancer: novel role of fumarate in regulation of HIF stability. In *Cancer Cell* (2005/08/16 ed., Vol. 8, pp. 143-153).

Izquierdo, M., Jimeno, J. F., & Lacuesta, A. (2015). *SPAIN: FROM IMMIGRATION TO EMIGRATION?* In B. d. Espana (Ed.), (Vol. 1503).

Jafri, M., & Maher, E. R. (2012). The genetics of phaeochromocytoma: using clinical features to guide genetic testing. In *Eur J Endocrinol* (2011/09/08 ed., Vol. 166, pp. 151-158).

Jochmanova, I., & Pacak, K. (2018). Genomic Landscape of Pheochromocytoma and Paraganglioma. In *Trends Cancer* (2018/02/08 ed., Vol. 4, pp. 6-9).

Jochmanova, I., Wolf, K. I., King, K. S., Nambuba, J., Wesley, R., Martucci, V.*, et al.* (2017). SDHB-related pheochromocytoma and paraganglioma penetrance and genotype-phenotype correlations. In *J Cancer Res Clin Oncol* (2017/04/05 ed., Vol. 143, pp. 1421-1435).

Jochmanova, I., Yang, C., Zhuang, Z., & Pacak, K. (2013). Hypoxia-inducible factor signaling in pheochromocytoma: turning the rudder in the right direction. In *J Natl Cancer Inst* (2013/08/14 ed., Vol. 105, pp. 1270-1283).

Juhlin, C. C., Stenman, A., Haglund, F., Clark, V. E., Brown, T. C., Baranoski, J.*, et al.* (2015). Whole-exome sequencing defines the mutational landscape of pheochromocytoma and identifies KMT2D as a recurrently mutated gene. In *Genes Chromosomes Cancer* (2015/06/03 ed., Vol. 54, pp. 542-554).

References

Katabathina, V. S., Rajebi, H., Chen, M., Restrepo, C. S., Salman, U., Vikram, R.*, et al.* (2019). Genetics and imaging of pheochromocytomas and paragangliomas: current update. In *Abdom Radiol (NY)* (2019/05/10 ed.).

Kent, W. J., Sugnet, C. W., Furey, T. S., Roskin, K. M., Pringle, T. H., Zahler, A. M.*, et al.* (2002). The human genome browser at UCSC. In *Genome Res* (2002/06/05 ed., Vol. 12, pp. 996-1006).

Kim, S., Cho, C. S., Han, K., & Lee, J. (2016). Structural Variation of Alu Element and Human Disease. In *Genomics Inform* (2016/10/13 ed., Vol. 14, pp. 70-77).

Kolomietz, E., Meyn, M. S., Pandita, A., & Squire, J. A. (2002). The role of Alu repeat clusters as mediators of recurrent chromosomal aberrations in tumors. In *Genes Chromosomes Cancer* (2002/08/31 ed., Vol. 35, pp. 97-112).

Ladroue, C., Carcenac, R., Leporrier, M., Gad, S., Le Hello, C., Galateau-Salle, F.*, et al.* (2008). PHD2 mutation and congenital erythrocytosis with paraganglioma. In *N Engl J Med* (2008/12/19 ed., Vol. 359, pp. 2685-2692).

Lam, A. K. (2017). Update on Adrenal Tumours in 2017 World Health Organization (WHO) of Endocrine Tumours. In *Endocr Pathol* (2017/05/10 ed., Vol. 28, pp. 213-227).

Latif, F., Tory, K., Gnarra, J., Yao, M., Duh, F. M., Orcutt, M. L.*, et al.* (1993). Identification of the von Hippel-Lindau disease tumor suppressor gene. In *Science* (1993/05/28 ed., Vol. 260, pp. 1317-1320).

Lefebvre, S., Borson-Chazot, F., Boutry-Kryza, N., Wion, N., Schillo, F., Peix, J. L.*, et al.* (2012). Screening of mutations in genes that predispose to hereditary paragangliomas and pheochromocytomas. In *Horm Metab Res* (2012/04/21 ed., Vol. 44, pp. 334-338).

Lenders, J. W., Duh, Q. Y., Eisenhofer, G., Gimenez-Roqueplo, A. P., Grebe, S. K., Murad, M. H.*, et al.* (2014). Pheochromocytoma and paraganglioma: an endocrine society clinical practice guideline. In *J Clin Endocrinol Metab* (2014/06/04 ed., Vol. 99, pp. 1915-1942).

Lenders, J. W., Eisenhofer, G., Mannelli, M., & Pacak, K. (2005). Phaeochromocytoma. In *Lancet* (2005/08/23 ed., Vol. 366, pp. 665-675).

Lodish, M. B., Adams, K. T., Huynh, T. T., Prodanov, T., Ling, A., Chen, C.*, et al.* (2010). Succinate dehydrogenase gene mutations are strongly associated with paraganglioma of the organ of Zuckerkandl. In *Endocr Relat Cancer* (2010/04/27 ed., Vol. 17, pp. 581-588).

Lodish, M. B., & Stratakis, C. A. (2008). RET oncogene in MEN2, MEN2B, MTC and other forms of thyroid cancer. In *Expert Rev Anticancer Ther* (2008/04/12 ed., Vol. 8, pp. 625-632).

Lorenzo, F. R., Yang, C., Ng Tang Fui, M., Vankayalapati, H., Zhuang, Z., Huynh, T.*, et al.* (2013). A novel EPAS1/HIF2A germline mutation in a congenital polycythemia with paraganglioma. In *J Mol Med (Berl)* (2012/10/24 ed., Vol. 91, pp. 507-512).

Maher, E. R., Neumann, H. P., & Richard, S. (2011). von Hippel-Lindau disease: a clinical and scientific review. In *Eur J Hum Genet* (2011/03/10 ed., Vol. 19, pp. 617-623).

Mannelli, M., Castellano, M., Schiavi, F., Filetti, S., Giacche, M., Mori, L.*, et al.* (2009). Clinically guided genetic screening in a large cohort of italian patients with pheochromocytomas and/or functional or nonfunctional paragangliomas. In *J Clin Endocrinol Metab* (2009/02/19 ed., Vol. 94, pp. 1541-1547).

Marini, F., Falchetti, A., Del Monte, F., Carbonell Sala, S., Gozzini, A., Luzi, E.*, et al.* (2006). Multiple endocrine neoplasia type 1. In *Orphanet J Rare Dis* (2006/10/04 ed., Vol. 1, pp. 38).

Martins, Calafell, F., Gaspar, C., Wong, V. C., Silveira, I., Nicholson, G. A.*, et al.* (2007). Asian origin for the worldwide-spread mutational event in Machado-Joseph disease. In *Arch Neurol* (2007/10/10 ed., Vol. 64, pp. 1502-1508).

Martins, Nunes, J. B., Maximo, V., Soares, P., Peixoto, J., Catarino, T.*, et al.* (2013). A founder SDHB mutation in Portuguese paraganglioma patients. In *Endocr Relat Cancer* (2013/10/05 ed., Vol. 20, pp. L23-26).

Martins, R., & Bugalho, M. J. (2014). Paragangliomas/Pheochromocytomas: clinically oriented genetic testing. In *Int J Endocrinol* (2014/06/06 ed., Vol. 2014, pp. 794187).

Matise, T. C., Chen, F., Chen, W., De La Vega, F. M., Hansen, M., He, C.*, et al.* (2007). A second-generation combined linkage physical map of the human genome. In *Genome Res* (2007/11/09 ed., Vol. 17, pp. 1783-1786).

McWhinney, S. R., Pilarski, R. T., Forrester, S. R., Schneider, M. C., Sarquis, M. M., Dias, E. P.*, et al.* (2004). Large germline deletions of mitochondrial complex II subunits SDHB and SDHD in hereditary paraganglioma. In *J Clin Endocrinol Metab* (2004/11/09 ed., Vol. 89, pp. 5694-5699).

Michalowska, I., Lewczuk, A., Cwikla, J., Prejbisz, A., Swoboda-Rydz, U., Furmanek, M. I.*, et al.* (2016). Evaluation of Head and Neck Paragangliomas by Computed Tomography in Patients with Pheochromocytoma-Paraganglioma Syndromes. In *Pol J Radiol* (2016/11/22 ed., Vol. 81, pp. 510-518).

Moraes, O. L. (2014). *DESCRIÇÃO CLÍNICA, IMUNOHISTOQUÍMICA E ESTUDO DOS GENES VHL, SDHB, SDHC, SDHD E MAX EM UMA SÉRIE DE PACIENTES COM FEOCROMOCITOMA E PARAGANGLIOMA DO DISTRITO FEDERAL.* (MSc), Universidade de Brasília, Brasília.

Mulligan, L. M., Kwok, J. B., Healey, C. S., Elsdon, M. J., Eng, C., Gardner, E.*, et al.* (1993). Germ-line mutations of the RET proto-oncogene in multiple endocrine neoplasia type 2A. In *Nature* (1993/06/03 ed., Vol. 363, pp. 458-460).

Muth, A., Crona, J., Gimm, O., Elmgren, A., Filipsson, K., Stenmark Askmalm, M.*, et al.* (2019). Genetic testing and surveillance guidelines in hereditary pheochromocytoma and paraganglioma. In *J Intern Med* (2018/12/12 ed., Vol. 285, pp. 187-204).

NCCN. (2019). National Comprehensive Cancer Network. Neuroendocrine and Adrenal Tumors (Version 1.2019) In.

Neary, N. M., King, K. S., & Pacak, K. (2011). Drugs and pheochromocytoma--don't be fooled by every elevated metanephrine. In *N Engl J Med* (2011/06/10 ed., Vol. 364, pp. 2268-2270).

Neumann, H. P., Erlic, Z., Boedeker, C. C., Rybicki, L. A., Robledo, M., Hermsen, M.*, et al.* (2009). Clinical predictors for germline mutations in head and neck paraganglioma patients: cost reduction strategy in genetic diagnostic process as fall-out. In *Cancer Res* (2009/04/09 ed., Vol. 69, pp. 3650-3656).

Neumann, H. P., Pawlu, C., Peczkowska, M., Bausch, B., McWhinney, S. R., Muresan, M.*, et al.* (2004). Distinct clinical features of paraganglioma syndromes associated with SDHB and SDHD gene mutations. In *JAMA* (2004/08/26 ed., Vol. 292, pp. 943-951).

Niemann, S., & Muller, U. (2000). Mutations in SDHC cause autosomal dominant paraganglioma, type 3. In *Nat Genet* (2000/11/04 ed., Vol. 26, pp. 268-270).

Opotowsky, A. R., Moko, L. E., Ginns, J., Rosenbaum, M., Greutmann, M., Aboulhosn, J., *et al.* (2015). Pheochromocytoma and paraganglioma in cyanotic congenital heart disease. In *J Clin Endocrinol Metab* (2015/01/13 ed., Vol. 100, pp. 1325-1334).

Pacak, K., Chrousos, G., Koch, C., Lenders, J., & Eisenhofer, G. (2001). Pheochromocytoma: progress in diagnosis, therapy, and genetics. . In C. G. Margioris A, editors (Ed.), *Adrenal Disorders* (1 ed., Vol. 1, pp. 479–523): Humana Press.

Pacak, K., Eisenhofer, G., & Ilias, I. (2009). Diagnosis of pheochromocytoma with special emphasis on MEN2 syndrome. In *Hormones (Athens)* (2009/07/03 ed., Vol. 8, pp. 111-116).

Pacak, K., & Tella, S. H. (2000). Pheochromocytoma and Paraganglioma. In K. R. Feingold, B. Anawalt, A. Boyce, G. Chrousos, K. Dungan, A. Grossman, J. M. Hershman, G. Kaltsas, C. Koch, P. Kopp, M. Korbonits, R. McLachlan, J. E. Morley, M. New, L. Perreault, J. Purnell, R. Rebar, F. Singer, D. L. Trence, A. Vinik, & D. P. Wilson (Eds.), *Endotext*. South Dartmouth (MA).

Pang, Y., Liu, Y., Pacak, K., & Yang, C. (2019). Pheochromocytomas and Paragangliomas: From Genetic Diversity to Targeted Therapies. In *Cancers (Basel)* (2019/03/31 ed., Vol. 11).

Parenti, G., Zampetti, B., Rapizzi, E., Ercolino, T., Giache, V., & Mannelli, M. (2012). Updated and new perspectives on diagnosis, prognosis, and therapy of malignant pheochromocytoma/paraganglioma. In *J Oncol* (2012/08/02 ed., Vol. 2012, pp. 872713).

Parrish, A., Caswell, R., Jones, G., Watson, M. C., Crinnion, A. L., & Ellard, S. (2017). An enhanced method for targeted next generation sequencing copy number variant detection using ExomeDepth [version 1; referees: 1 approved, 1 approved with reservations]. In *Wellcome Open Resarch 2017, 2:49*.

Plouin, P. F., Amar, L., Dekkers, O. M., Fassnacht, M., Gimenez-Roqueplo, A. P., Lenders, J. W.*, et al.* (2016). European Society of Endocrinology Clinical Practice Guideline for long-term follow-up of patients operated on for a phaeochromocytoma or a paraganglioma. In *Eur J Endocrinol* (2016/04/07 ed., Vol. 174, pp. G1-G10).

Qin, Y., Yao, L., King, E. E., Buddavarapu, K., Lenci, R. E., Chocron, E. S.*, et al.* (2010). Germline mutations in TMEM127 confer susceptibility to pheochromocytoma. In *Nat Genet* (2010/02/16 ed., Vol. 42, pp. 229-233).

Rattenberry, E., Vialard, L., Yeung, A., Bair, H., McKay, K., Jafri, M.*, et al.* (2013). A comprehensive next generation sequencing-based genetic testing strategy to improve diagnosis of inherited pheochromocytoma and paraganglioma. In *J Clin Endocrinol Metab* (2013/05/15 ed., Vol. 98, pp. E1248-1256).

Ricketts, C. J., Forman, J. R., Rattenberry, E., Bradshaw, N., Lalloo, F., Izatt, L.*, et al.* (2010). Tumor risks and genotype-phenotype-proteotype analysis in 358 patients with germline mutations in SDHB and SDHD. In *Hum Mutat* (2009/10/06 ed., Vol. 31, pp. 41-51).

Ricketts, C. J., Shuch, B., Vocke, C. D., Metwalli, A. R., Bratslavsky, G., Middelton, L.*, et al.* (2012). Succinate dehydrogenase kidney cancer: an aggressive example of the Warburg effect in cancer. In *J Urol* (2012/10/23 ed., Vol. 188, pp. 2063-2071).

Rijken, J. A., Niemeijer, N. D., Corssmit, E. P., Jonker, M. A., Leemans, C. R., Menko, F. H.*, et al.* (2016). Low penetrance of paraganglioma and pheochromocytoma in an extended kindred with a germline SDHB exon 3 deletion. In *Clin Genet* (2015/04/02 ed., Vol. 89, pp. 128-132).

Rijken, J. A., Niemeijer, N. D., Jonker, M. A., Eijkelenkamp, K., Jansen, J. C., van Berkel, A.*, et al.* (2018). The penetrance of paraganglioma and pheochromocytoma in SDHB germline mutation carriers. In *Clin Genet* (2017/05/16 ed., Vol. 93, pp. 60-66).

RORENO. (2016). Registo Oncológico Nacional 2010. Instituto Português de Oncologia do Porto Francisco Gentil - EPE. In. Porto.

Schiavi, F., Boedeker, C. C., Bausch, B., Peczkowska, M., Gomez, C. F., Strassburg, T.*, et al.* (2005). Predictors and prevalence of paraganglioma syndrome associated with mutations of the SDHC gene. In *JAMA* (2005/10/27 ed., Vol. 294, pp. 2057-2063).

Schiavi, F., Milne, R. L., Anda, E., Blay, P., Castellano, M., Opocher, G.*, et al.* (2010). Are we overestimating the penetrance of mutations in SDHB? In *Hum Mutat* (2010/06/01 ed., Vol. 31, pp. 761-762).

Seeley, R. R., Stephens, T. D., & Tate, P. (2006a). Autonomic Nervous System. In McGraw-Hill (Ed.), *Anatomy & Physiology* (pp. 562-566).

Seeley, R. R., Stephens, T. D., & Tate, P. (2006b). Functional Organization of Nervous Tissue. In McGraw-Hill (Ed.), *Anatomy & Physiology* (7th ed., pp. 374-403).

Shen, M. H., Harper, P. S., & Upadhyaya, M. (1996). Molecular genetics of neurofibromatosis type 1 (NF1). In *J Med Genet* (1996/01/01 ed., Vol. 33, pp. 2-17).

Shuch, B., Ricketts, C. J., Metwalli, A. R., Pacak, K., & Linehan, W. M. (2014). The genetic basis of pheochromocytoma and paraganglioma: implications for management. In *Urology* (2014/03/20 ed., Vol. 83, pp. 1225-1232).

Solis, D. C., Burnichon, N., Timmers, H. J., Raygada, M. J., Kozupa, A., Merino, M. J.*, et al.* (2009). Penetrance and clinical consequences of a gross SDHB deletion in a large family. In *Clin Genet* (2009/04/25 ed., Vol. 75, pp. 354-363).

Sousa, F., Martins, I., & Pereira, C. (2007). *A emigração Portuguesa para o Brasil.* (E. e. S. CEPESE – Centro de Estudos da População Ed. 1117 ed.). Porto, Portugal: Edições Afrontamento.

Timmers, H. J., Kozupa, A., Eisenhofer, G., Raygada, M., Adams, K. T., Solis, D.*, et al.* (2007). Clinical presentations, biochemical phenotypes, and genotype-phenotype correlations in patients with succinate dehydrogenase subunit B-associated pheochromocytomas and paragangliomas. In *J Clin Endocrinol Metab* (2007/01/04 ed., Vol. 92, pp. 779-786).

Toledo, R. A., Burnichon, N., Cascon, A., Benn, D. E., Bayley, J. P., Welander, J.*, et al.* (2017). Consensus Statement on next-generation-sequencing-based diagnostic testing of hereditary phaeochromocytomas and paragangliomas. In *Nat Rev Endocrinol* (2016/11/20 ed., Vol. 13, pp. 233-247).

Tufton, N., Shapiro, L., Sahdev, A., Kumar, A. V., Martin, L., Drake, W. M.*, et al.* (2019). An analysis of surveillance screening for SDHB-related disease in childhood and adolescence. In *Endocr Connect* (2019/01/30 ed., Vol. 8, pp. 162-172).

Turchini, J., Cheung, V. K. Y., Tischler, A. S., De Krijger, R. R., & Gill, A. J. (2018). Pathology and genetics of phaeochromocytoma and paraganglioma. In *Histopathology* (2017/12/15 ed., Vol. 72, pp. 97-105).

Wadt, K., Choi, J., Chung, J. Y., Kiilgaard, J., Heegaard, S., Drzewiecki, K. T.*, et al.* (2012). A cryptic BAP1 splice mutation in a family with uveal and cutaneous melanoma, and paraganglioma. In *Pigment Cell Melanoma Res* (2012/08/15 ed., Vol. 25, pp. 815-818).

Waguespack, S. G., Rich, T., Grubbs, E., Ying, A. K., Perrier, N. D., Ayala-Ramirez, M.*, et al.* (2010). A current review of the etiology, diagnosis, and treatment of pediatric pheochromocytoma and paraganglioma. In *J Clin Endocrinol Metab* (2010/03/11 ed., Vol. 95, pp. 2023-2037).

Wang, Y. M., Gu, M. L., & Ji, F. (2015). Succinate dehydrogenase-deficient gastrointestinal stromal tumors. In *World J Gastroenterol* (2015/03/06 ed., Vol. 21, pp. 2303-2314).

Weber, A., Hoffmann, M. M., Neumann, H. P., & Erlic, Z. (2012). Somatic mutation analysis of the SDHB, SDHC, SDHD, and RET genes in the clinical assessment of sporadic and hereditary pheochromocytoma. In *Horm Cancer* (2012/05/11 ed., Vol. 3, pp. 187-192).

Wehrwein, E. A., Orer, H. S., & Barman, S. M. (2016). Overview of the Anatomy, Physiology, and Pharmacology of the Autonomic Nervous System. In *Compr Physiol* (2016/06/28 ed., Vol. 6, pp. 1239-1278).

Wohllk, N., Schweizer, H., Erlic, Z., Schmid, K. W., Walz, M. K., Raue, F.*, et al.* (2010). Multiple endocrine neoplasia type 2. In *Best Pract Res Clin Endocrinol Metab* (2010/09/14 ed., Vol. 24, pp. 371-387).

Xekouki, P., Szarek, E., Bullova, P., Giubellino, A., Quezado, M., Mastroyannis, S. A.*, et al.* (2015). Pituitary adenoma with paraganglioma/pheochromocytoma (3PAs) and succinate dehydrogenase defects in humans and mice. In *J Clin Endocrinol Metab* (2015/02/20 ed., Vol. 100, pp. E710-719).

Xu, W., Mulligan, L. M., Ponder, M. A., Liu, L., Smith, B. A., Mathew, C. G.*, et al.* (1992). Loss of NF1 alleles in phaeochromocytomas from patients with type I neurofibromatosis. In *Genes Chromosomes Cancer* (1992/06/01 ed., Vol. 4, pp. 337-342).

Yang, C., Zhuang, Z., Fliedner, S. M., Shankavaram, U., Sun, M. G., Bullova, P.*, et al.* (2015). Germ-line PHD1 and PHD2 mutations detected in patients with pheochromocytoma/paraganglioma-polycythemia. In *J Mol Med (Berl)* (2014/09/30 ed., Vol. 93, pp. 93-104).

Yeh, I. T., Lenci, R. E., Qin, Y., Buddavarapu, K., Ligon, A. H., Leteurtre, E.*, et al.* (2008). A germline mutation of the KIF1B beta gene on 1p36 in a family with neural and nonneural tumors. In *Hum Genet* (2008/08/30 ed., Vol. 124, pp. 279-285).